

# Kosterlitz-Thouless transition in thin films: A Monte Carlo study of three-dimensional lattice models

Martin Hasenbusch

*Institut für Theoretische Physik, Universität Leipzig*  
*Postfach 100 920, D-04009 Leipzig, Germany*  
*e-mail: Martin.Hasenbusch@itp.uni-leipzig.de*

## Abstract

We study the phase transition of thin films in the three-dimensional XY universality class. To this end, we perform a Monte Carlo study of the improved two-component  $\phi^4$  model, the improved dynamically diluted XY model and the standard XY model on the simple cubic lattice. We study films of a thickness up to  $L_0 = 32$  lattice spacings. In the short direction of the lattice free boundary conditions are employed. Using a finite size scaling (FSS) method, proposed recently, we determine the transition temperature with high accuracy. The effectively two-dimensional finite size scaling behaviour of the Binder cumulant  $U_4$ , the second moment correlation length over the lattice size  $\xi_{2nd}/L$ , the ratio of the partition functions with anti-periodic and periodic boundary conditions  $Z_a/Z_p$  and the helicity modulus  $\Upsilon$  clearly confirm the Kosterlitz-Thouless nature of the transition. We analyse the scaling of the transition temperature with the thickness  $L_0$  of the film. The predictions of the renormalization group (RG) theory are confirmed. We compute the universal ratio of the thickness of the film  $L_0$  and the transversal correlation length  $\xi_T$  in the three-dimensional thermodynamic limit at the Kosterlitz-Thouless transition temperature of a film of thickness  $L_0$ :  $[L_{0,KT}/\xi_T]^* = 1.595(7)$ . This results can be compared with experimental results on thin films of  $^4\text{He}$  near the  $\lambda$ -transition.

**Keywords:**  $\lambda$ -transition, Classical Monte Carlo simulation, thin films

# 1 Introduction

In the neighbourhood of a second order phase transition the correlation length diverges as

$$\xi \simeq f_{\pm}|t|^{-\nu}, \quad (1)$$

where  $t = (T - T_c)/T_c$  is the reduced temperature,  $f_+$  and  $f_-$  are the amplitudes in the high and the low temperature phase, respectively, and  $\nu$  is the critical exponent of the correlation length. In the neighbourhood of the transition also the behaviour of other quantities is governed by power laws. E.g. the specific heat behaves as

$$C \simeq A_{\pm}|t|^{-\alpha} + B, \quad (2)$$

where  $B$  is an analytic background, which has to be taken into account here, since the critical exponent  $\alpha$  of the specific heat is negative for the three-dimensional XY universality class, as we shall see below. Critical exponents like  $\nu$  and  $\alpha$  and ratios of amplitudes such as  $f_+/f_-$  and  $A_+/A_-$  assume universal values. I.e. they are supposed to assume exactly the same value for any system in a given universality class. This can be understood in the framework of the Renormalization Group (RG). A universality class is characterised by the dimension of the system, the range of the interaction and the symmetry of the order parameter. For reviews on critical phenomena and the Renormalization Group see e.g. [1, 2, 3, 4].

At temperatures below the  $\lambda$ -transition,  $^4\text{He}$  becomes superfluid. The order parameter of the  $\lambda$ -transition is the phase of a wave function. Therefore it is supposed to share the three-dimensional XY universality class, which is characterized by the  $O(2)$ , or equivalently  $U(1)$ , symmetry of the order parameter. The most accurate experimental results for critical exponents and amplitude ratios are obtained for the  $\lambda$ -transition of  $^4\text{He}$ . E.g. under the condition of micro-gravity, the specific heat has been studied for reduced temperatures as small as  $t \approx 5 \times 10^{-10}$  [5, 6], resulting in  $\alpha = -0.0127(3)$ , corresponding to  $\nu = 0.6709(1)$ . Note that the exponents of the specific heat and the correlation length are related via the hyperscaling relation  $d\nu = 2 - \alpha$ , where  $d$  is the dimension of the system. Experiments on earth, measuring the specific heat and the second sound to obtain the superfluid density have resulted in accurate estimates of the exponent of the correlation length  $\nu = 0.6717(4)$  and  $\nu = 0.6705(6)$  in refs. [7, 8], respectively. For a recent review and an outlook on future experiments in space-stations, see ref. [9]. The experimental results for critical exponents are in reasonable agreement with the most precise theoretical prediction for the three-dimensional XY universality class:  $\nu = 0.6717(1)$  obtained from a combined Monte Carlo and high temperature

series study of improved lattice models [10]. For a summary of theoretical results obtained with various methods (e.g. field-theoretic methods) see ref. [4]. Also in the case of universal amplitude ratios, there is reasonable match between theoretical results for the three-dimensional XY universality class and experimental studies of the  $\lambda$ -transition. See refs. [11, 12] and refs. therein.

The discussion above refers to the thermodynamic limit. It is a natural question how the behaviour at the transition is altered by a finite extension of the system. It has been addressed both experimentally and theoretically. In systems with a finite extension in all directions, there can not be any singularity such as eqs. (1,2). As a remnant of these singularities there remains a peak in the neighbourhood of the transition. With increasing linear extension the height of the peak increases and the temperature of the maximum approaches the critical temperature.

The situation might be different, if the extension in some of the directions stays infinite. In the case of one infinite direction and two finite ones the system becomes effectively one-dimensional. For the type of interactions that we are dealing with here, there is no phase transition at a finite temperature for a one-dimensional system. Hence one expects that the behaviour of the effectively one-dimensional system is qualitatively the same as that of a system which is finite in all directions.

In the case of a thin film geometry, i.e. one direction with finite extension and two infinite ones, we expect that the system becomes effectively two-dimensional in the neighbourhood of the transition. Hence, there will be still a phase transition, however it belongs to the two-dimensional universality class. I.e. in our case of U(1) symmetry of the order parameter, a Kosterlitz-Thouless (KT) transition [13, 14, 15] is expected.

The behaviour of finite systems in the neighbourhood of a continuous transition is described by finite size scaling (FSS). For a reviews see [16, 17]. In essence, close to the transition the bulk correlation length  $\xi$ , i.e. the correlation length in the three-dimensional thermodynamic limit, and the extension of the finite system are the only relevant length scales. I.e. the physics of finite systems is governed by the ratio  $L_0/\xi$ . In particular, one expects that, independent on the thickness  $L_0$  of the thin film, the effectively two-dimensional phase transition occurs at a universal value of  $L_0/\xi$ . One should note that this universal value depends on the type of boundary conditions that are applied in the finite direction of the system. Using eq. (1) it follows that [18, 19]

$$T_{c,3d} - T_{KT}(L_0) \simeq L_0^{-1/\nu} \quad , \quad (3)$$

where  $T_{c,3d}$  is the transition temperature of the three-dimensional system and  $T_{KT}(L_0)$  the temperature of the KT transition of the thin film of thickness  $L_0$ .

The predictions of finite size scaling have been checked by various explicit calculations and experiments [16, 17]. For a recent review of experimental results near the  $\lambda$ -transition of  $^4\text{He}$  and  $^3\text{He}$ - $^4\text{He}$  mixtures see [20]. For thin films in the three-dimensional XY universality class a multitude of field theoretic calculations have been performed which allow for comparison with experiment [21]. Some important aspects of the behaviour of thin films are however not accessible using field theoretic methods. Among these is the KT transition, which is the focus of the present work.

In thin films of  $^4\text{He}$  on various substrates, the order parameter is vanishing at the boundary of the film. This has to be taken into account in the Monte Carlo simulation of lattice models with film geometry. The simplest way to obtain a vanishing field at the boundary are so called free boundary conditions. For a precise definition see the section below. An alternative are so called staggered boundary conditions. The numerical results of ref. [22] confirm that free and staggered boundary conditions lead the same results for universal quantities.

On top of the restricted geometry, free boundary conditions might introduce new physical effects; For reviews on surface critical phenomena see refs. [23, 24]. In fact, free boundary conditions lead to additional corrections to scaling. The leading one is  $\propto L_0^{-1}$  [25]; it can be cast in the form  $L_{0,eff} = L_0 + L_s$ . These corrections come in addition to those  $\propto L_0^{-\omega}$ ,  $\propto L_0^{-\omega'}$ , ..., which are predicted for finite systems in general, irrespective of the type of the boundary conditions [16]. Note that the numerical value of the correction exponent is  $\omega = 0.785(20)$  [10]; similar results are obtained with field-theoretic methods; see e.g. the review [4]. The information on  $\omega'$  is rather sparse; following ref. [26]  $\omega' \approx 2\omega$ . Fitting Monte Carlo data, it might be difficult to disentangle corrections  $\propto L_0^{-\omega}$  and  $\propto L_0^{-1}$ , leading to sizable errors in the extrapolation  $L_0 \rightarrow \infty$ . In order to avoid this problem, and to clearly show the existence of corrections  $\propto L_0^{-1}$  due to the free boundary conditions, we have studied improved models. In these models the amplitude of corrections  $\propto L_0^{-\omega}$  vanishes, or in practise, it is so small that its effect can be ignored. The precise definition of these models is given below.

In the literature on can find only a few Monte Carlo studies of lattice models that address the scaling of the KT temperature with the thickness of the film. Janke and Nather [27] have studied the Villain model on the simple cubic lattice with free boundary conditions in the short direction. They have determined the temperature of the KT transition from the behaviour of the correlation length and the magnetic susceptibility in the high temperature phase of the thin films. They have studied films of a thickness up to  $L_0 = 16$ . Fitting the transition temperature with eq. (3) they find a value for the exponent  $\nu$  that is about 5% too large compared with the estimates of  $\nu$  discussed above.

Schultka and Manousakis [28] have studied the standard XY model with periodic boundary conditions in all directions. They studied lattices up to a thickness  $L_0 = 10$ . They determined the KT transition temperature using the effectively two-dimensional finite size scaling behaviour of the helicity modulus. They conclude that their results are consistent with eq. (3), using  $\nu = 0.6705$ , which was the best experimental estimate of the correlation length exponent at the time. The same authors [29, 30] have studied the standard XY model with staggered boundary conditions in the short direction. Also in this case, they have determined the KT transition temperature using the effectively two-dimensional finite size scaling behaviour of the helicity modulus. They studied films of the thicknesses  $L_0 = 4, 8, 12, 16$  and  $20$ . They find that their data can be fitted with eq. (3) using  $\nu = 0.6705$ . However in this case, that requires that  $L_0$  in eq. (3) is replaced by  $L_{0,eff} = L_0 + L_s$ , with  $L_s = 5.79(50)$ . They have also reanalysed the data of ref. [27] this way. They find that also these results are compatible with  $\nu = 0.6705$ , once  $L_0$  is replaced by  $L_{0,eff}$  with  $L_s = 1.05(2)$ . One should note however that Schultka and Manousakis do not take into account corrections  $\propto L_0^{-\omega}$  which should be present in the standard XY as well as in the Villain model.

There are further Monte Carlo studies of thin films using lattice models in the three-dimensional XY universality class. These studies focus on the specific heat [22] and refs. therein, the thermal resistivity [31] and refs. therein, or the thermodynamic Casimir force [32, 33]. Throughout, the thickness of the films that had been studied is less or equal to  $L_0 = 24$ .

This paper is organized as follows: In the following section, we define the lattice models that we have studied. Then we introduce the observables that we have measured. In section 5 we study the effect of free boundary conditions in finite size scaling (FSS) directly at the critical temperature of the three dimensional system. In section 6 we briefly summarize the method proposed in ref. [34] to determine the KT transition temperature. Then we determine the KT transition temperature for a large range of the thickness of the film. We demonstrate that the transition of the thin films is indeed of KT nature. To this end we compare the behaviour of various phenomenological couplings, also called dimensionless quantities in the following, at the transition temperature with predictions from KT theory and from numerical results for two-dimensional systems that are known to undergo a KT transition. Next we study the scaling behaviour of the KT transition temperature with the thickness of the film. Then we compute universal amplitude ratios that relate the thickness of the film with the correlation length of the bulk system at the temperature of the KT transition of the thin film. We compare our estimate for the universal amplitude ratio with that of experiments on thin films of  ${}^4\text{He}$ .

## 2 The models

We study various models with  $O(2)$ -symmetry on a simple cubic lattice. We consider systems with film geometry. We shall label the sites of the lattice by  $x = (x_0, x_1, x_2)$ . The components of  $x$  might assume the values  $x_i \in \{1, 2, \dots, L_i\}$ . We simulate lattices of the size  $L_1 = L_2 = L$  and  $L_0 \ll L$ . In 1 and 2-direction we employ periodic boundary conditions and free boundary conditions in 0-direction. This means that the sites with  $x_0 = 1$  and  $x_0 = L_0$  have only five nearest neighbours. This type of boundary condition could also be interpreted as Dirichlet boundary conditions with 0 as value of the field at  $x_0 = 0$  and  $x_0 = L_0 + 1$ .

The standard XY model is given by the Hamiltonian

$$\mathcal{H}_{XY} = -\beta \sum_{\langle x,y \rangle} \vec{s}_x \vec{s}_y, \quad (4)$$

where  $\vec{s}_x$  is a unit-vector in  $\mathbb{R}^2$ .  $\langle x, y \rangle$  denotes a pair of nearest neighbour sites on the lattice. In our convention, the inverse temperature  $\beta$  is absorbed into the Hamiltonian. The Boltzmann factor is given by  $\exp(-\mathcal{H}_{XY})$ . The best estimates of the inverse transition temperature that are quoted in the literature are  $\beta_c = 0.454165(4)$ ,  $0.454167(4)$ ,  $0.4541659(10)$  and  $0.4541652(11)$  in refs. [35, 36, 37, 10], respectively. In the following we shall assume  $\beta_c = 0.4541655(10)$  which is, roughly, the average of the estimates given by refs. [37, 10].

A generalization of the XY model is the  $\phi^4$  model on the lattice. The Hamiltonian is given by

$$\mathcal{H}_{\phi^4} = -\beta \sum_{\langle x,y \rangle} \vec{\phi}_x \cdot \vec{\phi}_y + \sum_x \left[ \vec{\phi}_x^2 + \lambda(\vec{\phi}_x^2 - 1)^2 \right], \quad (5)$$

where the field variable  $\vec{\phi}_x$  is a vector with two real components. The partition function is given by

$$Z_{\phi^4} = \prod_x \left[ \int d\phi_x^{(1)} \int d\phi_x^{(2)} \right] \exp(-\mathcal{H}_{\phi^4}). \quad (6)$$

In the limit  $\lambda \rightarrow \infty$  the field is fixed to unit length; i.e. the XY model is recovered. For  $\lambda = 0$  we get the exactly solvable Gaussian model. For  $0 < \lambda \leq \infty$  the model undergoes a second order transition that belongs to the XY universality class. For a discussion see e.g. [38]. Numerically, using Monte Carlo simulations and high-temperature series expansions, it has been shown that there is a value

$\lambda^* > 0$ , where leading corrections to scaling vanish. Numerical estimates of  $\lambda^*$  given in the literature are  $\lambda^* = 2.10(6)$  [39],  $\lambda^* = 2.07(5)$  [40] and most recently  $\lambda^* = 2.15(5)$  [10]. The inverse of the transition temperature has been determined accurately for several values of  $\lambda$  using finite size scaling (FSS) [10]. We shall perform our simulations at  $\lambda = 2.1$ , since for this value of  $\lambda$  comprehensive Monte Carlo studies of the three dimensional system in the low and the high temperature phase have been performed [10, 11, 12]. The inverse critical temperature at  $\lambda = 2.1$  is  $\beta_c = 0.5091503(6)$  [10]. Since  $\lambda = 2.1$  is not exactly equal to  $\lambda^*$ , there are still corrections  $\propto L^{-\omega}$ , although with a small amplitude. In fact, following ref. [10], it should be by at least a factor 20 smaller than for the standard XY model.

The dynamically diluted XY model [40, 10] is given by

$$\mathcal{H}_{\text{ddXY}} = -\beta \sum_{\langle xy \rangle} \vec{\phi}_x \cdot \vec{\phi}_y - D \sum_x \vec{\phi}_x^2 \quad (7)$$

with the local measure

$$d\mu(\phi_x) = d\phi_x^{(1)} d\phi_x^{(2)} \left[ \delta(\phi_x^{(1)}) \delta(\phi_x^{(2)}) + \frac{1}{2\pi} \delta(1 - |\vec{\phi}_x|) \right], \quad (8)$$

i.e.  $|\vec{\phi}_x|$  is either 0 or 1, and the partition function

$$Z_{\text{ddXY}} = \int \prod_x d\mu(\phi_x) \exp(-\mathcal{H}_{\text{ddXY}}) . \quad (9)$$

In the limit  $D \rightarrow \infty$  the standard XY model is recovered. For  $D < D_{tri}$  the model undergoes a first order transition and for  $D > D_{tri}$  a second order transition in the XY universality class. A mean-field calculation gives  $D_{tri} = 0$ , while from a improved mean-field calculation we get  $D_{tri} < 0$  [40]. Therefore it is quite save to assume that indeed  $D_{tri} < 0$  for the ddXY model.

From Monte Carlo simulations and high temperature series expansion we know that there is a  $D_{tri} < D^* < \infty$  such that leading corrections to scaling vanish. Numerical estimates are  $D^* = 1.02(3)$  [40] and  $D^* = 1.06(2)$  [10]. Here we shall present some preliminary results for  $D = 1.02$ . At this value of  $D$ , the inverse critical temperature is  $\beta_c = 0.5637963(4)$ . Also here, the amplitude of leading corrections to scaling should be by at least a factor 20 smaller than for the standard XY model [10].

### 3 The observables

The total magnetisation is defined by

$$\vec{M} = \sum_x \vec{\phi}_x . \quad (10)$$

Note that in the case of the XY model we have to replace  $\vec{\phi}_x$  by  $\vec{s}_x$  here and in the following definitions. The magnetic susceptibility in the high temperature phase, for vanishing external field, is given by

$$\chi = \frac{1}{L_0 L_1 L_2} \langle \vec{M}^2 \rangle , \quad (11)$$

where  $\langle \dots \rangle$  denotes the expectation value with respect to the Boltzmann factors defined in the previous section. The Binder cumulant is defined by

$$U_4 = \frac{\langle (\vec{M}^2)^2 \rangle}{\langle \vec{M}^2 \rangle^2} . \quad (12)$$

We also consider the generalization

$$U_6 = \frac{\langle (\vec{M}^2)^3 \rangle}{\langle \vec{M}^2 \rangle^3} . \quad (13)$$

We have computed the second moment correlation length for the 1- and 2-direction (i.e. the large ones). The second moment correlation length in 1-direction is defined by

$$\xi_{2nd,1} = \sqrt{\frac{\chi/F_1 - 1}{4 \sin(\pi/L_1)^2}} , \quad (14)$$

where

$$F_1 = \frac{1}{L_0 L_1 L_2} \left\langle \left| \sum_x \exp\left(i \frac{2\pi x_1}{L_1}\right) \vec{\phi}_x \right|^2 \right\rangle \quad (15)$$

is the Fourier transform of the correlation function at the lowest non-zero momentum in 1-direction. In our simulations, we also have measured  $F_2$  in order to reduce the statistical error.

The helicity modulus  $\Upsilon$  gives the reaction of the system under a torsion. To define the helicity modulus we consider a system, where rotated boundary conditions



are introduced in one direction: For  $x_1 = L_1$  and  $y_1 = 1$  the term  $\vec{\phi}_x \vec{\phi}_y$  in the Hamiltonian is replaced by

$$\vec{\phi}_x \cdot R_\alpha \vec{\phi}_y = \phi_x^{(1)} (\cos(\alpha)\phi_y^{(1)} + \sin(\alpha)\phi_y^{(2)}) + \phi_x^{(2)} (-\sin(\alpha)\phi_y^{(1)} + \cos(\alpha)\phi_y^{(2)}) \quad . \quad (16)$$

The helicity modulus is then given by

$$\Upsilon = -\frac{L_1}{L_0 L_2} \frac{\partial^2 \log Z(\alpha)}{\partial \alpha^2} \Big|_{\alpha=0} \quad . \quad (17)$$

Note that we have skipped a factor of  $T$  compared with the standard definition [42]. Defined this way, the helicity modulus has the dimension of an inverse length. In the literature  $\xi_\perp = 1/\Upsilon$  is referred to as transversal correlation length. The helicity modulus can be directly evaluated in the Monte Carlo simulation. Following eq. (3) of ref. [41] one gets for the models considered here

$$\Upsilon = \frac{\beta}{L_0 L_1 L_2} \left\langle \sum_x \vec{\phi}_x \vec{\phi}_{x+(0,1,0)} \right\rangle - \frac{\beta^2}{L_0 L_1 L_2} \left\langle \left[ \sum_x (\phi_x^{(1)} \phi_{x+(0,1,0)}^{(2)} - \phi_x^{(2)} \phi_{x+(0,1,0)}^{(1)}) \right]^2 \right\rangle \quad . \quad (18)$$

In addition we have measured the analogous quantity for the 2-direction. A problem of the estimator (18) of  $\Upsilon$  is that for a fixed number of measurements and  $L_i \Upsilon$  fixed, the statistical error is increasing as the critical point is approached; see e.g. ref. [12]. In section 4 below we shall discuss how this problem can be reduced to some extent. From the definition (17) one reads off that  $L_0 \Upsilon$  is dimensionless. Therefore, in the case of thin films the behaviour of  $L_0 \Upsilon$  has to be compared with the prediction for two-dimensional systems in the neighbourhood of the Kosterlitz-Thouless transition.

The ratio of partition functions  $Z_a/Z_p$  is a useful quantity in the numerical study of phase transitions. Here  $Z_p$  is the partition function of a system with periodic boundary conditions in two directions of the lattice and free boundary conditions in the remaining direction, while  $Z_a$  is the partition function of a system with anti-periodic boundary conditions in one of the directions and periodic and free boundary conditions in the other two directions. Anti-periodic means that, e.g. in the 1-direction, at the boundary, i.e. for  $x_1 = L_1$  and  $y_1 = 1$  the term  $\vec{\phi}_x \vec{\phi}_y$  is replaced by  $-\vec{\phi}_x \vec{\phi}_y$  in the Hamiltonian. This can also be viewed as a rotation by  $\pi$ . The ratio of partition functions can be efficiently measured in Monte Carlo simulations using a special version of the cluster algorithm [43]. The implementation of the algorithm that is used here follows the discussion given in Appendix A 2. of ref. [40].

## 4 The Monte Carlo Algorithm

For our simulations we use a composition of local and cluster algorithms. The implementation is similar to that used in ref. [40]. See Appendix A 1. of ref. [40] for details. Applied to the standard XY model cluster algorithms are ergodic. However, in the case of the ddXY model and the  $\phi^4$  model additional local updates are needed to change  $|\phi_x|$ . As cluster algorithms, we have used both the single-cluster [44] and the wall-cluster algorithm [45].

Let us briefly discuss the details of the local updates for the case of the  $\phi^4$  model for which most of our simulations were performed. In the case of the Metropolis update a proposal is generated as

$$\begin{aligned}\phi_x^{(1)'} &= \phi_x^{(1)} + s \left( r - \frac{1}{2} \right) \\ \phi_x^{(2)'} &= \frac{3}{4} \beta \Phi_x^{(2)} - \phi_x^{(2)}\end{aligned}\tag{19}$$

with  $s = 3$  (the choice of  $s$  is such that very roughly the acceptance rate is 50%) and

$$\vec{\Phi}_x = \sum_{y.nn.x} \vec{\phi}_y ,\tag{20}$$

where  $y.nn.x$  means that  $y$  is a nearest neighbour of  $x$ . The idea of this proposal is to change also the second component without using a random number. The probability to accept this proposal is  $P_{acc} = \min[1, \exp(-\Delta H)]$ . This update is followed by a second one at the same site, where the role of the two components is exchanged. Using these updates we run through the lattice in typewriter fashion. Going through the lattice once is referred to as one sweep in the following.

We have also implemented overrelaxation updates for all models that we have simulated. These are given by

$$\vec{\phi}_x' = \vec{\phi}_x - 2 \frac{\vec{\Phi}_x \cdot \vec{\phi}_x}{\vec{\Phi}_x^2} \vec{\Phi}_x ,\tag{21}$$

where

$$\vec{\Phi}_x = \sum_{y.nn.x} \vec{\phi}_y .\tag{22}$$

Note that these updates do not change the value of the Hamiltonian and therefore no accept/reject step is needed. Hence it is computationally quite cheap since no

random number and no evaluation of  $\exp()$  is needed. Also in the case of the overrelaxation update we run through the lattice in typewriter fashion. As the cluster updates, the overrelaxation update does not change  $|\phi_x|$ . The main motivation to use the overrelaxation update is that it allows to reduce the variance problem of the helicity modulus to some extent. Since the overrelaxation update is quite cheap in terms of CPU-time, we performed several sweeps with the overrelaxation update in each update cycle. After each of these sweeps the second term on the right hand side of eq. (18) is measured. For a lack of human time we did not carefully tune the number of overrelaxation sweeps per update cycle.

As random number generator we have used the SIMD-oriented Fast Mersenne Twister (SFMT) [46] generator. In particular, we use the `genrand_res53()` function that produces double-precision output.

## 5 Finite size scaling at $\beta_{c,3d}$

First we performed simulations at the transition temperature of the three-dimensional system. This way we avoid possible difficulties related with the KT transition and hence can see more clearly the effects caused by free boundary conditions. Corrections caused by the free boundaries should qualitatively not depend on  $L_1$  and  $L_2$ , as long as  $L_1$  and  $L_2$  scale with  $L_0$ . Therefore we consider lattices with  $L_0 \approx L_1 = L_2$ , allowing us to study a relatively large range in  $L_0$ .

We have simulated the  $\phi^4$  model at  $\lambda = 2.1$  at the best estimate of the inverse of the critical temperature of the three-dimensional system:  $\beta = 0.5091503$  [10]. We consider the lattice sizes  $L_1 = L_2 = 8, 12, 16, 24, 32$  and 48. In addition to  $L_0 = L_1$  we have simulated  $L_0 = L_1 - 1$ . Throughout we have performed  $10^8$  measurements. For each of these measurements, one boundary flip update, several single cluster updates, one Metropolis sweep, and three overrelaxation sweeps were performed. Note that this composition is essentially chosen ad hoc. In total, these simulations took about 6 month of CPU time on one core of a Xeon(R) CPU 5160 running at 3 GHz. We have measured the dimensionless quantities  $Z_a/Z_p$ ,  $\xi_{2nd}/L$ ,  $U_4$  and  $U_6$  as defined in section 3. For all these quantities we have determined the coefficients of the Taylor series in  $\beta$  around  $\beta = 0.5091503$  up to third order. This allows us to evaluate these quantities in the neighbourhood of  $\beta = 0.5091503$ . Our results for  $Z_a/Z_p$  and  $\xi_{2nd}/L$  are plotted in figure 1. The results for  $U_4$  and  $U_6$  are given in figure 2. In the case of  $L_0 = L_1$  corrections are clearly visible for all four quantities considered. Plotted as a function of  $1/L_1$ , the data for  $L_0 = L_1$  follow roughly a straight line, indicating that the corrections are proportional to  $L_1^{-1}$ , as expected.

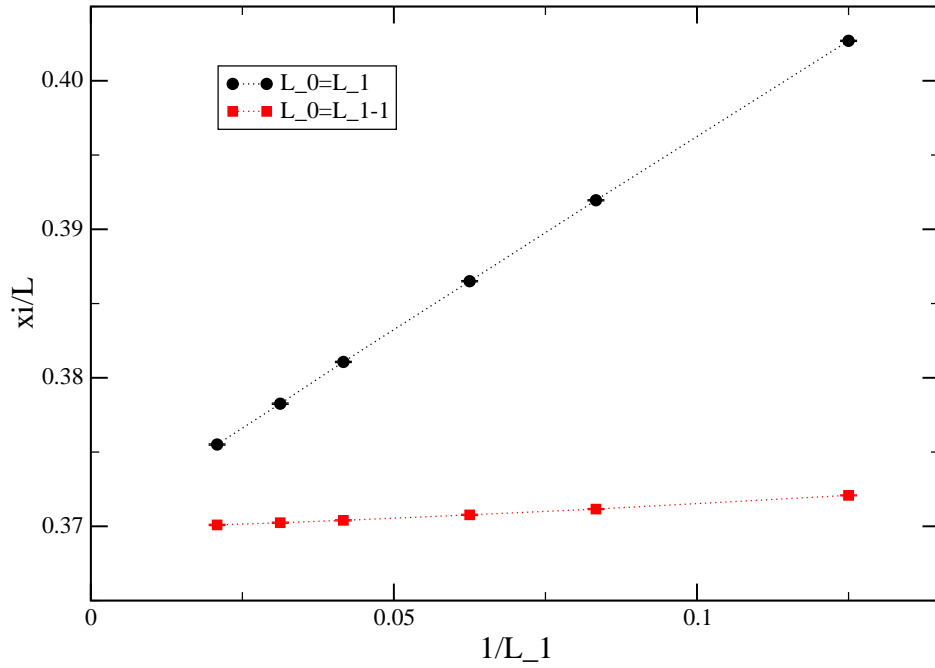
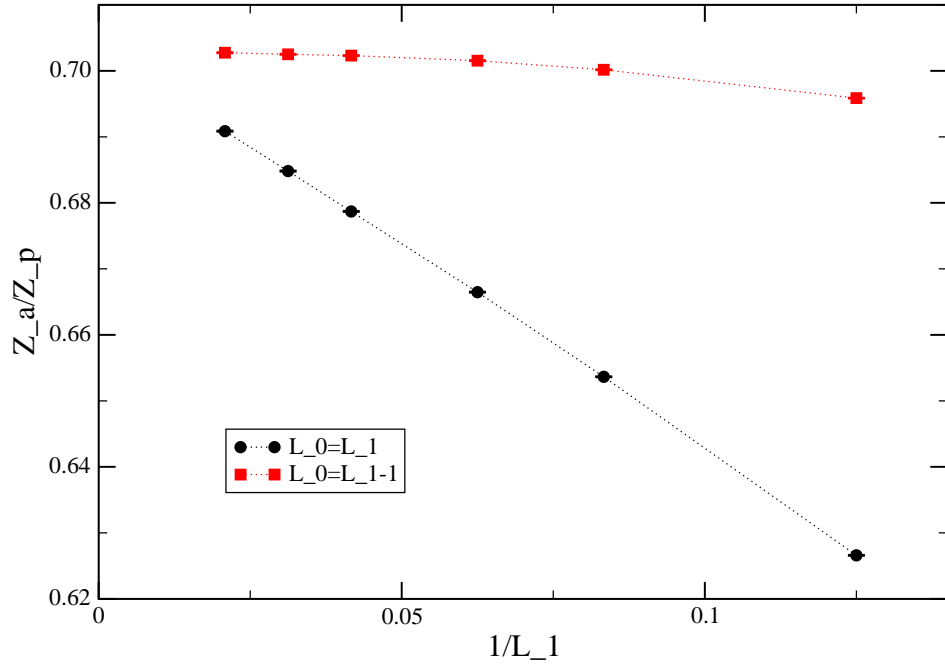
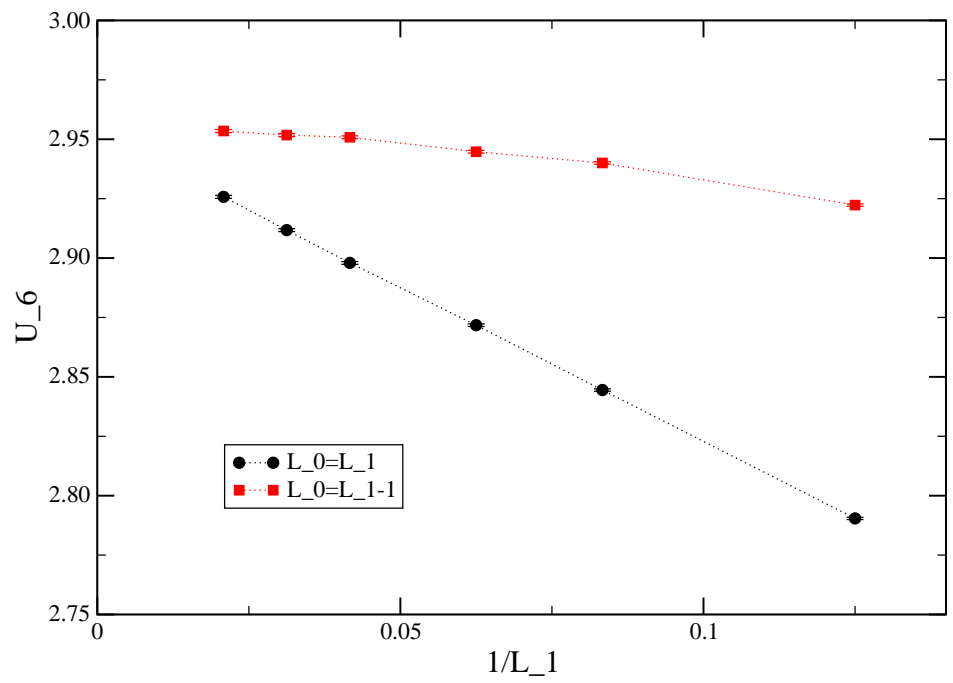
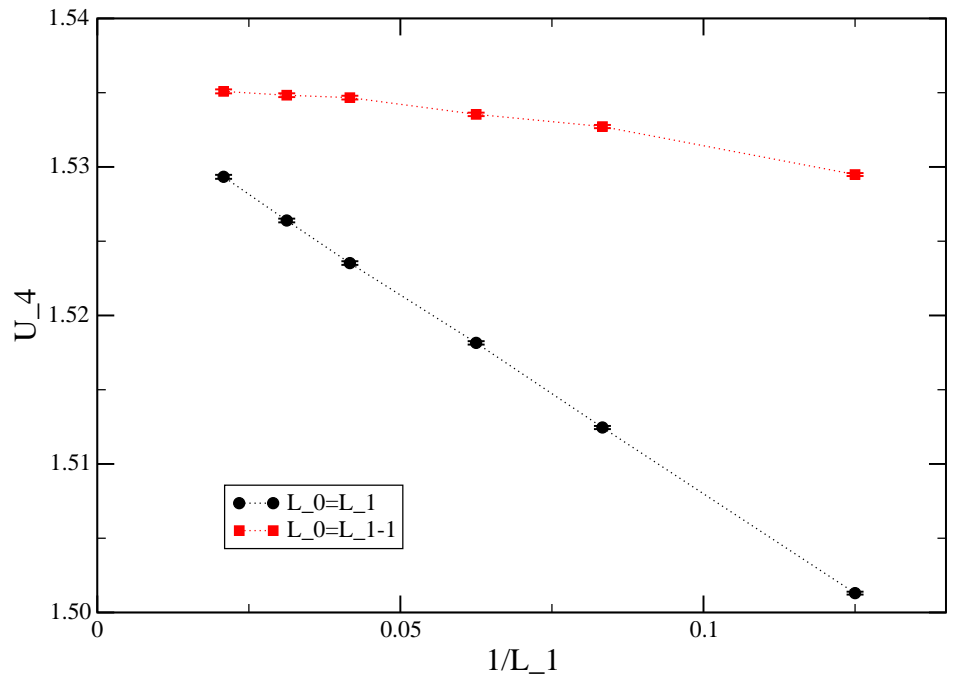


Figure 1: The  $\phi^4$  model at  $\lambda = 2.1$  and  $\beta = 0.5091503$ . The upper (lower) figure gives  $Z_a/Z_p$  ( $\xi_{2nd}/L$ ) as a function of  $1/L_1$ . We have simulated systems with  $L_0 = L_1 = L_2$  and  $L_0 + 1 = L_1 = L_2$ .



12  
 Figure 2: Same as previous figure, but for  $U_4$  and  $U_6$ .

Table 1: Fits of  $Z_a/Z_p$  with the ansatz (23).  $L_{1,min}$  is the minimal lattice size included into the fit. For a discussion see the text.

$L_{1,min}$	$(Z_a/Z_p)^*$	$L_s$	$\chi^2/\text{d.o.f.}$
8	0.70474(4)	1.117(1)	111.45
12	0.70364(5)	1.068(2)	11.84
16	0.70326(7)	1.046(3)	1.68
24	0.70311(12)	1.033(7)	0.18

Table 2: Fits of  $\xi_{2nd}/L$  with the ansatz (23).  $L_{1,min}$  is the minimal lattice size included into the fit. For a discussion see the text.

$L_{1,min}$	$(\xi_{2nd}/L)^*$	$L_s$	$\chi^2/\text{d.o.f.}$
8	0.36988(2)	1.066(1)	16.97
12	0.36988(3)	1.058(2)	4.98
16	0.36988(4)	1.053(4)	2.80
24	0.36986(7)	1.049(8)	0.51

In addition, we give results for lattices with  $L_0 = L_1 - 1$ . Here, for the largest values of  $L_1$ , the curves are almost flat for all quantities considered. E.g. the plots suggest that the dominant corrections can be explained by an effective thickness  $L_{0,eff} = L_0 + L_s$  with  $L_s \approx 1$ .

In the following we put this discussion on a more quantitative level by performing a sequence of fits of our data for the dimensionless quantities.

First we have fitted the dimensionless quantities with the ansatz

$$R(L_1, L_1 - L_0) = R^* + c(L_1 - L_0)L_1^{-1} \quad , \quad (23)$$

where  $R^*$ ,  $c(0)$  and  $c(1)$  are the parameters of the fit.  $L_s$  is given by the zero of  $c(L_1 - L_0)$ . Using our data, we have linearly interpolated/extrapolated  $c(0)$  and  $c(1)$  resulting in

$$L_s = \frac{c(0)}{c(0) - c(1)} \quad . \quad (24)$$

Results of such fits are given in the tables 1, 2, 3 and 4 for  $Z_a/Z_p$ ,  $\xi_{2nd}/L$ ,  $U_4$  and  $U_6$ , respectively.

Table 3: Fits of  $U_4$  with the ansatz (23).  $L_{1,min}$  is the minimal lattice size included into the fit. For a discussion see the text.

$L_{1,min}$	$U_4^*$	$L_s$	$\chi^2/\text{d.o.f.}$
8	1.53578(7)	1.188(5)	28.39
12	1.53545(9)	1.119(7)	7.57
16	1.53540(12)	1.097(12)	6.49
24	1.53531(20)	1.055(24)	0.31

Table 4: Fits of  $U_6$  with the ansatz (23).  $L_{1,min}$  is the minimal lattice size included into the fit. For a discussion see the text.

$L_{1,min}$	$U_6^*$	$L_s$	$\chi^2/\text{d.o.f.}$
8	2.9573(3)	1.224(5)	33.83
12	2.9556(5)	1.145(8)	8.57
16	2.9553(6)	1.119(12)	6.84
24	2.9547(10)	1.070(24)	0.63

In all four cases, an acceptable  $\chi^2/\text{d.o.f.}$  is only reached for  $L_{1,\min} = 24$ . From the fits with  $L_{1,\min} = 24$  we get quite consistent results for  $L_s$  for the four quantities considered. They range from  $L_s = 1.033(7)$  for  $Z_a/Z_p$  up to  $L_s = 1.070(24)$  for  $U_6$ .

In order to check the possible error due to the uncertainty of  $\beta_c$ , we have repeated the fits for  $L_{1,\min} = 24$  for  $\beta = 0.5091509$ . The result for e.g.  $Z_a/Z_p$  is  $(Z_a/Z_p)^* = 0.70294(12)$  and  $L_s = 1.0277(7)$ . I.e. the effect is of similar size as the statistical error.

Next we performed fits with the ansatz

$$R(L_1, L_1 - L_0) = R^* + c_1(L_1 - L_0)L_1^{-1} + c_2(L_1 - L_0)L_1^{-2} \quad , \quad (25)$$

where now  $R^*$ ,  $c_1(0)$ ,  $c_1(1)$ ,  $c_2(0)$  and  $c_2(1)$  are the free parameters of the fit. Here we have not included explicitly  $L^{-\omega'}$  corrections, since at the level of our numerical resolution  $\omega'$  is rather close to 2.

Using this ansatz, we get  $\chi^2/\text{d.o.f.} \approx 1$  already for  $L_{1,\min} = 8$  for all four quantities that we study. The results for  $L_s$  from these fits are slightly smaller than those from the ansatz (25):  $L_s = 0.955(5), 1.040(6), 0.991(19)$  and  $0.998(18)$  from  $Z_a/Z_p$ ,  $\xi_{2nd}/L$ ,  $U_4$  and  $U_6$ , respectively. In the case of  $Z_a/Z_p$ , where the result for  $L_s$  is the smallest, we get  $L_s = 0.969(11)$  from  $L_{1,\min} = 12$ . I.e. it is moving towards the other results. Also here, we have checked the effect of the uncertainty in  $\beta_c$ . E.g. for  $\beta_c = 0.5091509$  and  $L_{1,\min} = 8$  one obtains  $L_s = 0.950(5), 1.035(7), 0.981(18)$ , and  $0.988(18)$ , from  $Z_a/Z_p$ ,  $\xi_{2nd}/L$ ,  $U_4$  and  $U_6$ , respectively. I.e. the effect is of similar size as the statistical error at fixed  $\beta$ .

As our final result we quote

$$L_s = 1.02(7) \quad (26)$$

where the error-bar covers all the results of the fits reported above.

Here we did not explicitly check the possible error due to residual corrections  $\propto L^{-\omega}$  at  $\lambda = 2.1$ . However, corrections  $\propto L^{-\omega}$  should affect different phenomenological couplings in a different way. Therefore the variation of  $L_s$  obtained from different quantities should also provide an estimate of the error resulting from residual corrections  $\propto L^{-\omega}$ .

Our final values for the fixed point values of the dimensionless quantities are  $(Z_a/Z_p)^* = 0.7030(5)$ ,  $(\xi_{2nd}/L)^* = 0.36986(10)$ ,  $U_4^* = 1.5352(2)$ , and  $U_6^* = 2.954(1)$ . These values can be compared with those of a  $L^3$  system with periodic boundary conditions in all three directions [10]:  $(Z_a/Z_p)^* = 0.3203(1)[3]$ ,  $(\xi_{2nd}/L)^* = 0.5924(1)[3]$ ,  $U_4^* = 1.2431(1)[1]$ , and  $U_6 = 1.7509(2)[7]$ , where the number in  $[\ ]$  gives



the systematic error due to scaling corrections. The effect of the boundary conditions is very well visible. In the case of  $(Z_a/Z_p)^*$  the value even differs by more than a factor of two.

The numbers quoted here, could be used to check whether other boundary conditions, e.g. staggered boundary conditions, are equivalent with free boundary conditions. One would expect a different value of  $L_s$  but the same values of  $R^*$  for equivalent boundary conditions.

## 6 Finite size scaling at the KT transition

Finite size scaling is an efficient method to locate and to verify the nature of the KT transition in two-dimensional systems. To this end, usually the helicity modulus  $\Upsilon$  is studied. Following ref. [47] it behaves as

$$\Upsilon = \frac{2}{\pi} + \frac{1}{\pi} \frac{1}{(\ln L + C)} \dots \quad (27)$$

at the transition temperature. Recently, we have pointed out [48] that for lattices with periodic boundary conditions there are numerically small contributions from winding configurations that are not taken into account in eq. (27). Including these contributions one gets [48]

$$\Upsilon_{L^2,transition} = 0.63650817819\dots + \frac{0.318899454\dots}{\ln L + C} + \dots \quad (28)$$

for an  $L^2$  lattice with periodic boundary conditions in both directions at the KT transition. In the appendix we derive for the ratio of partition functions

$$(Z_a/Z_p)_{L^2,transition} = 0.0864272337\dots - \frac{0.135755793\dots}{\ln L + C} + \dots \quad (29)$$

for an  $L^2$  lattice at the KT transition. We have also determined the leading finite size behaviour of the second moment correlation length over the lattice size [48]

$$\left. \frac{\xi_{2nd}}{L} \right|_{L^2,transition} = 0.7506912\dots + \frac{0.212430\dots}{\ln L + C} + \dots \quad (30)$$

and more recently for the Binder cumulant [34]

$$U_{4,L^2,transition} = 1.018192(6) - \frac{0.017922(5)}{\ln L + C} + \dots \quad (31)$$

Eqs. (28, 30) describe quite well the behaviour of numerical data for  $\Upsilon$  and  $\xi_{2nd}/L$  for various models down to rather small lattice sizes. In contrast to that, on the accessible lattice sizes,  $U_4$  is decreasing with increasing  $L$ , while eq. (31) suggests that it should increase. This behaviour is explained by disorder caused by vortex pairs at a distance of the order  $L/2$ . Therefore a term  $c_2/(\ln L + C)^2$  has been added to eq. (31). The coefficient  $c_2$  and  $C$  have been determined from fits to Monte Carlo data. The result for  $c_2$  is consistent for different models. This confirms the assumption that also the subleading correction in the Binder cumulant is universal [34].

In ref. [34] we suggest that the KT transition of a model can be accurately determined by matching  $\xi_{2nd}/L$  and the Binder cumulant  $U_4$  with that obtained from a model where  $\beta_{KT}$  is accurately known. In ref. [34] we have studied most accurately the dual of the absolute value solid-on-solid (ASOS) model. In this model, the KT transition occurs at  $\tilde{\beta} = 0.80608(2)$  [49].

The data of the dual of the ASOS model for  $L \geq 96$  are well described by

$$\begin{aligned} \tilde{\beta} &= 0.80608 \quad : \\ U_{4,ASOS}(L) &= 1.018192 - \frac{0.017922}{\ln L - 1.18} + \frac{0.06769}{(\ln L - 1.18)^2} \\ \frac{\xi_{2nd,ASOS}(L)}{L} &= 0.7506912 + \frac{0.212430}{\ln L + 0.573} . \end{aligned} \quad (32)$$

To check the error due to the uncertainty of  $\tilde{\beta}_{KT}$  one should repeat the matching with

$$\begin{aligned} \tilde{\beta} &= 0.80606 \quad : \\ U_{4,ASOS}(L) &= 1.018192 - \frac{0.017922}{\ln L - 1.193} + \frac{0.06730}{(\ln L - 1.193)^2} \\ \frac{\xi_{2nd,ASOS}(L)}{L} &= 0.7506912 + \frac{0.212430}{\ln L + 0.557} . \end{aligned} \quad (33)$$

In order to match the thin films with these expressions one has to adjust  $\beta$  and a scale factor for the lattice size.

## 7 KT transition in thin films

Here we have studied the KT transition of thin films of the  $\phi^4$  model at  $\lambda = 2.1$  using the matching method discussed above. We have simulated lattices of the thickness

$L_0 = 4, 6, 8, 12, 16, 24$  and  $32$ . In order to get the phenomenological couplings as functions of  $\beta$  we have computed the Taylor series of these quantities around  $\beta_s$  up to the third order, where in the simulation the configurations are generated with a Boltzmann factor corresponding to  $\beta_s$ . Since the Taylor expansion provides accurate results only in a small neighbourhood of  $\beta_s$ , we tried to chose  $\beta_s \approx \beta_{KT}(L_1)$ , where  $\beta_{KT}(L_1)$  is the solution of eqs. (32) for the given lattice size  $L_1$ . To this end, we performed some preliminary simulations or we extrapolated the result for  $\beta_{KT}(L_1)$  from small lattice sizes  $L_1$  to large ones. We carefully checked that in our final simulations the differences  $\beta_{KT}(L_1) - \beta_s$  are small enough to ensure that the Taylor series evaluated at  $\beta_{KT}(L_1)$  are sufficiently accurate for our purpose.

In our final simulations, mostly, we performed  $2 \times 10^6$  measurements. Only in the case our largest lattice,  $32 \times 1024^2$ , we only measured  $1.4 \times 10^6$  times. For each measurement, we performed single cluster updates, boundary flip updates and 3 overrelaxation sweeps and one Metropolis sweep. The number of single cluster updates was chosen such that, on average, the lattice is covered once by the clusters.

E.g. for the  $32 \times 1024^2$  lattice, the integrated autocorrelation time of the magnetic susceptibility is  $\tau_\chi \approx 0.7$ . I.e. individual measurements are almost statistically independent. The total CPU time used for these simulations was roughly the equivalent of 9 years on a single core of a 2.6 GHz Opteron CPU. Our results obtained from the matching with the dual of the ASOS model at  $\tilde{\beta} = 0.80608$  are summarized in table 5.

For all values of  $L_0$ ,  $\beta_{KT}(L_1)$  is decreasing with increasing  $L_1$ . Apparently the results are converging; The difference  $\beta_{KT}(L_1) - \beta_{KT}(2L_1)$  is decreasing with increasing  $L_1$ . For  $L_0 = 4$  and  $6$ , where we have the largest range of lattice sizes available, the differences of the results for  $L_1/L_0 = 64$  and  $L_1/L_0 = 128$  are already smaller than the error-bars.

Eqs. (32) are supposed to give the universal behaviour within the numerical precision that has been reached in ref. [34]. Corrections to the universal behaviour are expected to decay with a power of  $L_1$ , possibly multiplied by some power of  $\ln L_1$ . There are certainly corrections with an exponent  $\epsilon = 7/4$  due to the analytic background in the magnetic susceptibility. Furthermore there are corrections due to irrelevant scaling fields.

In order to check these expectations, we have fitted our estimates of  $\beta_{KT}(L_1)$  for  $L_0 = 4$  and  $6$ , where we have the largest values of  $L_1/L_0$  available, with the ansatz

$$\beta_{KT}(L_1) = \beta_{KT}(\infty) + cL_1^{-\epsilon} \quad , \quad (34)$$

where  $\beta_{KT}(\infty)$ ,  $c$  and  $\epsilon$  are the free parameters of the fit. The results of these fits are summarized in table 6. The numerical results for the correction exponent  $\epsilon$  are

Table 5: Matching the thin film with the dual of the ASOS model at  $\tilde{\beta} = 0.80608$ , eqs. (32). The parameters of the matching are the inverse KT temperature  $\beta_{KT}$  of the thin film and the lattice size  $L_{ASOS}$  of the dual of the ASOS model.

$L_0$	$L_1$	$\beta_{KT}$	$L_{ASOS}$
4	32	0.610518(24)	27.91(8)
4	64	0.609984(18)	53.9(3)
4	128	0.609784(17)	113.9(1.3)
4	256	0.609688(12)	227.9(3.3)
4	512	0.609699(11)	469.(12.)
6	48	0.568772(14)	30.38(10)
6	96	0.568453(12)	60.37(36)
6	192	0.568313(8)	125.1(1.4)
6	384	0.568262(7)	260.4(4.6)
6	768	0.568259(7)	544.(18.)
8	64	0.549585(9)	31.76(12)
8	128	0.549381(6)	63.6(4)
8	256	0.549314(5)	133.1(1.5)
8	512	0.549283(5)	272.8(5.5)
12	96	0.5322567(52)	33.06(12)
12	192	0.5321416(48)	65.9(6)
12	384	0.5321010(33)	139.6(1.8)
12	768	0.5320864(28)	297.6(6.6)
16	128	0.5245609(34)	33.87(13)
16	256	0.5244956(27)	67.5(5)
16	512	0.5244626(23)	140.5(1.8)
16	1024	0.5244547(19)	296.9(6.1)
24	192	0.5177878(19)	34.39(13)
24	384	0.5177446(15)	68.48(48)
24	768	0.5177340(11)	143.6(1.6)
32	256	0.5148522(12)	34.88(13)
32	512	0.5148259(9)	70.4(4)
32	1024	0.5148147(9)	147.7(2.2)

Table 6: Results of fits with the ansatz (34).  $L_{1,min}$  is the smallest lattice size that has been included into the fit. For a discussion see the text.

$L_0$	$L_{1,min}$	$\beta_{KT}(\infty)$	$c$	$\epsilon$	$\chi^2/\text{d.o.f.}$
4	32	0.609669(11)	0.14(4)	1.47(9)	2.78
4	64	0.609681(13)	0.6(6)	1.8(3)	4.31
6	48	0.568241(8)	0.12(4)	1.40(9)	1.48
6	96	0.568250(8)	0.6(8)	1.8(3)	0.94

Table 7: Matching the thin film with the dual of the ASOS model at  $\tilde{\beta} = 0.80606$ , eqs. (33). As examples we give the results for  $L_0 = 4$  and 6.

$L_0$	$L_1$	$\beta_{KT}$	$L_{ASOS}$
4	32	0.610532(24)	28.08(9)
4	64	0.609996(18)	54.1(3)
4	128	0.609793(17)	114.0(1.3)
4	256	0.609695(12)	227.7(3.2)
4	512	0.609705(11)	467.(12.)
6	48	0.568780(14)	30.57(10)
6	96	0.568459(12)	60.59(36)
6	192	0.568318(8)	125.3(1.4)
6	384	0.568266(7)	260.1(4.6)
6	768	0.568262(7)	542.(18.)

not very precise; they are essentially consistent with a leading correction exponent  $\epsilon = 7/4$  due to the analytic background in the magnetic susceptibility.

In order to check the uncertainty of our results for  $\beta_{KT}$  caused by the uncertainty of the estimate of the KT transition temperature in the ASOS model, we have repeated the matching with eqs. (33). As examples we give the results obtain for  $L_0 = 4$  and  $L_0 = 6$  in table 7.

We find that the difference in  $\beta_{KT}$  compared with the matching with eqs. (32) is smaller than the statistical error of  $\beta_{KT}$ . Also in the case of the matching lattice size  $L_{ASOS}$  of the ASOS model the difference is small. These observations also hold for larger values of  $L_0$  not given in table 7.

Table 8: Final results for the inverse KT transition temperature  $\beta_{KT}$  of thin films of the thickness  $L_0$ . The statistical error is given in () while the systematic one is quoted in []. For a discussion see the text. In addition we give in the last row the inverse critical temperature of the three dimensional system.

$L_0$	$\beta_{KT}$
4	0.60968(1)[1]
6	0.56825(1)[1]
8	0.549278(5)[9]
12	0.532082(3)[5]
16	0.524450(2)[3]
24	0.517730(2)[2]
32	0.514810(1)[2]
$\infty$	0.5091503(6)

As our final estimate of the inverse KT transition temperature for  $L_0 = 4$  we take  $\beta_{KT} = 0.60968(1)[1]$ , which is the result of the fit with the ansatz (34) using  $L_{1,min} = 64$ . The number given in [] is an estimate of the systematic error. It is estimated from the difference of the fit with the ansatz (34) using  $L_{1,min} = 32$  and  $L_{1,min} = 64$ . Furthermore we take into account the difference between the matching with eqs. (32) and eqs. (33). In a similar way we arrive at  $\beta_{KT} = 0.56825(1)[1]$  for  $L_0 = 6$ .

For  $L_0 \geq 8$  the range of  $L_1/L_0$  that we have simulated is smaller than for  $L_0 = 4$  and 6. Therefore, for these values of  $L_0$ , we use  $\epsilon = 7/4$  fixed in our fits (34) to obtain  $\beta_{KT}$  in the limit  $L_1/L_0 \rightarrow \infty$ . In all cases we did not include the smallest lattice size,  $L_1/L_0 = 8$ , into the fit. Even if  $\epsilon = 7/4$  is the dominant correction, subleading corrections will cause systematic errors. To estimate these, we assume that the effective correction exponent might take a value in the range  $1.5 < \epsilon < 2$  as it is suggest by our fits for  $L_0 = 4$  and 6. To this end, fitting with the ansatz (34) we have used  $\epsilon = 1.5$  in addition to  $\epsilon = 1.75$ . The systematic error is then estimated by the difference of these two fits. As a further check of systematic errors, we have repeated these fits for the estimates of  $\beta_{KT}$  obtained from the matching with the dual of the ASOS model at  $\tilde{\beta} = 0.80606$ , eqs. (33). Our final results are summarized in table 8.

From the matching of the thin films with the dual of the ASOS model, we obtain also a scale factor that relates the lattice size of the thin films and the dual of the

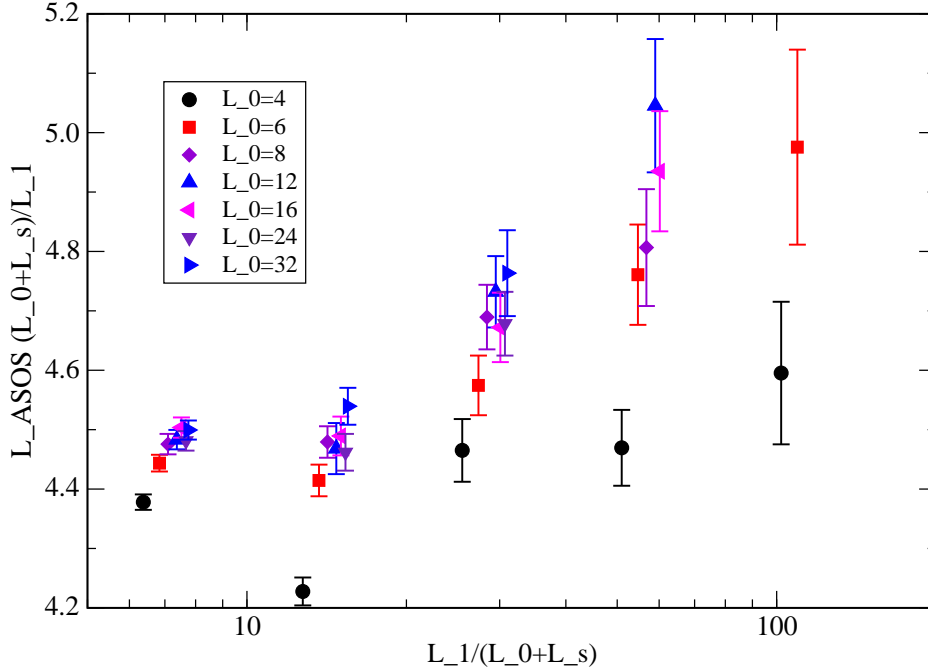


Figure 3: In the figure we give the matching factor  $(L_0 + L_s)L_{ASOS}/L_1$  between thin films and the dual of the ASOS model.

ASOS model. Following the RG prediction, thin films of different thickness  $L_0$  match, up to corrections to scaling, for the same values of  $L_1/(L_0 + L_s)$ .

In figure 3 we have plotted the matching factor

$$b_{ASOS, film} = L_{ASOS}(L_0 + L_s)/L_1 \quad (35)$$

between the dual of the ASOS model and thin films, where we have used  $L_s = 1.02$ , eq. (26). Starting from  $L_0 = 6$  the results for the same  $L_1/L_0$  are consistent among different  $L_0$ , confirming the RG prediction. The results for the scale factor are all in the range  $4.2 < b_{ASOS, film} < 5.2$ . Unfortunately, the statistical error increases a lot with increasing  $L_1/L_0$ . Also the value of the scale factor  $b_{ASOS, film}$  is still increasing for our largest values of  $L_1/L_0$ . Taking into account this trend, we shall assume

$$b_{ASOS, film} = 5.0(5) \quad (36)$$

as estimate for the limit  $L_1/L_0 \rightarrow \infty$  in the following.

Using the matching factors between the dual of the ASOS model and other XY models that are given in ref. [49], we arrive at

$$\begin{aligned}
b_{XY, film} &= L_{XY}L_0/L_1 = 1.7(2) \\
b_{Villain, film} &= L_{Villain}L_0/L_1 = 0.58(6) \\
b_{BCSOS, film} &= L_{BCSOS}L_0/L_1 = 1.8(2) .
\end{aligned}
\tag{37}$$

In the following we like to further check that the thin films indeed undergo a Kosterlitz-Thouless transition. In figure 4 we give  $U_4$  and  $\xi_{2nd}/L$  at the estimates of  $\beta_{KT}$  given in table 8 as a function of  $L_1/(L_0 + L_s)$ , where we use  $L_s = 1.02$ , eq. (26). For comparison we also give the results for the dual of the ASOS model represented by eqs. (32). In this case,  $U_4$  and  $\xi_{2nd}/L$  are plotted versus  $L_{ASOS}/b_{ASOS, film}$ , using  $b_{ASOS, film} = 5$ . The data for thin films with different  $L_0$  fall nicely on top of each other. This is even true for our smallest values of  $L_1/L_0$ . The thin film results do match nicely with those of the ASOS model only for the larger values of  $L_1/L_0$ . The approach of the thin film results to those of the ASOS model seems compatible with power law corrections. This behaviour is, of course, directly related with the behaviour of  $\beta_{KT}(L_1)$  obtained from the matching of  $U_4$  and  $\xi_{2nd}/L$ . Also there we have seen sizable corrections for small values of  $L_1/L_0$  that could be fitted by a power law.

In figure 5 we give our results for the ratio of partition functions  $Z_a/Z_p$  and the helicity modulus  $\Upsilon$ . In contrast to  $\xi_{2nd}/L$  and  $U_4$  these quantities have not been used to determine  $\beta_{KT}$ . Therefore they provide an additional check of the reliability of our results for  $\beta_{KT}$  and the matching factor  $b_{ASOS, film}$ . Also in the case of  $Z_a/Z_p$  the data for different values of  $L_0$  fall reasonably well on top of each other. Unfortunately we have no data for  $Z_a/Z_p$  for a two-dimensional XY model available. Therefore we can only compare with the leading behaviour, eq. (69), at the KT transition that we derive in the appendix. We determined the constant  $C$  by a 1-parameter fit of our data for  $L_0 = 16$  using  $L_1 = 512$  and  $L_1 = 1024$ , where we have used  $L = L_1/(L_0 + L_s)$ . The result is  $C = 4.31(7)$ . The result of this fit is given in the upper part of figure 5 by the dashed purple line.

In the lower part of figure 5 we give  $L_0\Upsilon$ . Note that, in contrast to section 7.2, the  $\Upsilon$  used here is measured on the thin films. The results for different  $L_0$  fall nicely on top of each other. As expected, the relative error of  $L_0\Upsilon$  increases with increasing thickness  $L_0$  of the film. For comparison we also plot results obtained for the 2D XY model [34]. We have plotted results for  $L_{XY} = 12, 16, 24, 32, 48, 64, 96, 128, 192$  and  $256$  as a function of  $L = L_{XY}/b_{XY, film}$ . The dashed line only connects the points to guide the eye. Here we find an almost perfect matching between the thin films



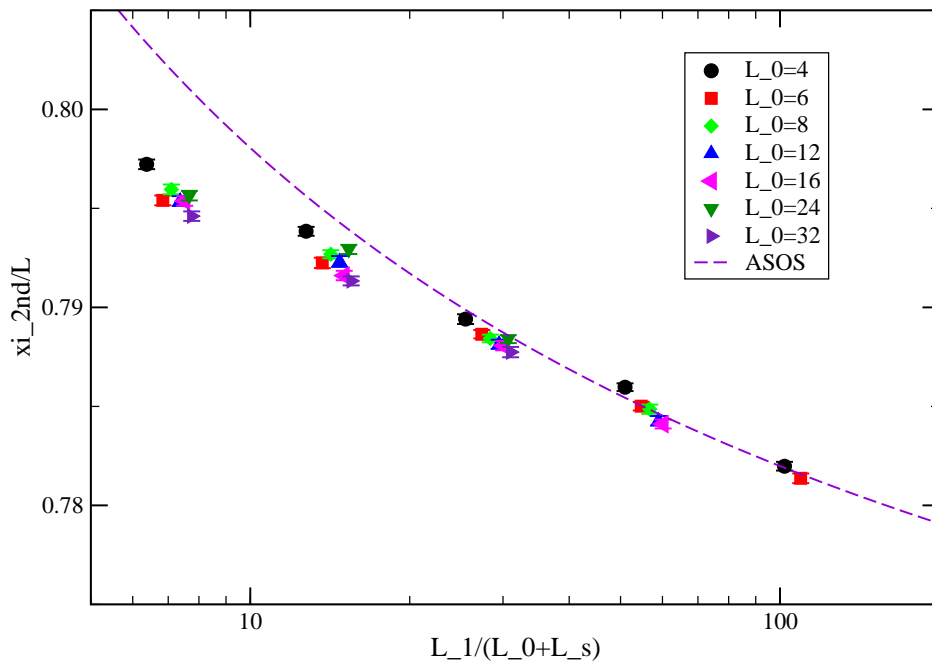
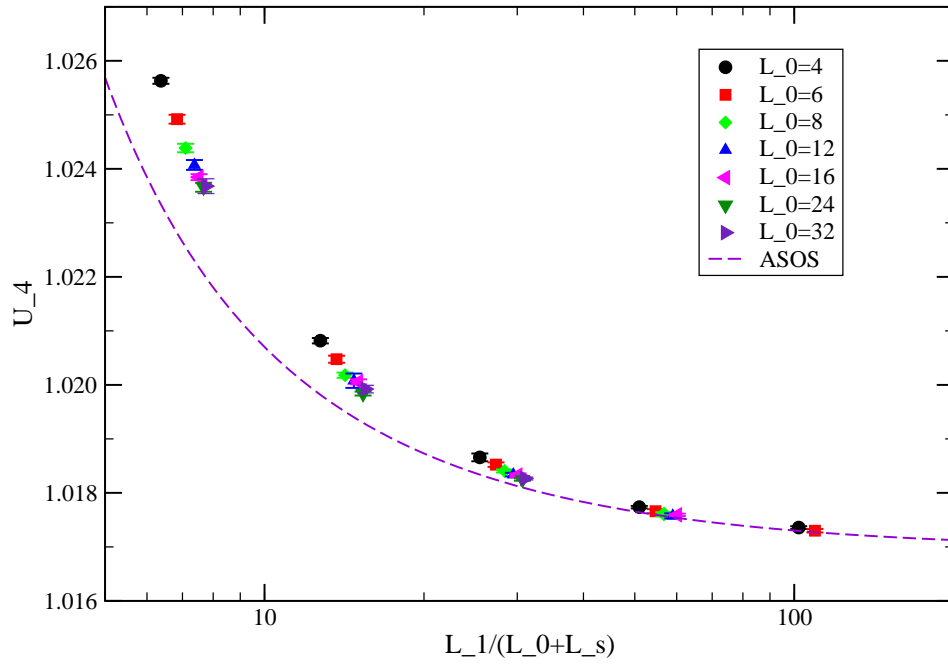


Figure 4: Effectively two-dimensional finite size scaling of  $U_4$  (upper part of the figure) and  $\xi_{2nd}/L$  (lower part of the figure). For a discussion see the text.

and the two-dimensional XY model, starting from our smallest values of  $L_1/L_0$ . This suggests that corrections to the universal KT behaviour are very small in the helicity modulus.

## 7.1 Scaling of $\beta_{KT}$ with $L_0$

As the thickness  $L_0$  increases, the KT transition temperature of the thin film approaches the transition temperature of the three-dimensional system. Finite size scaling predicts that this approach is governed by eq. (3), or equivalently in terms of the inverse temperature

$$\beta_{KT}(L_0) - \beta_{c,3d} \simeq L_0^{-1/\nu} . \quad (38)$$

Indeed from table 8 we read off that  $\beta_{KT}$  is approaching  $\beta_{c,3d}$  as  $L_0$  is increasing. In order to check whether this approach is compatible with a power law and in particular with the predicted exponent, we have computed

$$\nu_{eff,\beta}(L_0) = -\ln(2)/\ln\left(\frac{\beta_{KT}(2L_0) - \beta_{c,3d}}{\beta_{KT}(L_0) - \beta_{c,3d}}\right) , \quad (39)$$

where we use  $\beta_{c,3d} = 0.5091503(6)$  [10]. Analogously we define  $\nu_{eff,T}(L_0)$ , where in eq. (39)  $\beta_{KT} - \beta_{c,3d}$  is replaced by  $T_{KT} - T_{c,3d}$ . In the limit  $L_0 \rightarrow \infty$  both definitions give, by construction, the same result. Our results based on the numerical estimates of  $\beta_{KT}$  given in table 8 are plotted in figure 6. Note that the error-bars are smaller than the symbols. For simplicity we have added the systematic and the statistical error that is given in table 8. Also the error due to the uncertainty of  $\beta_{c,3d}$  is taken into account.

Our results for  $\nu_{eff,\beta}(L_0)$  and  $\nu_{eff,T}(L_0)$  differ quite a lot, indicating that analytic corrections are still important for the values of  $L_0$  considered. In both cases the effective exponent is decreasing with increasing  $L_0$ . Even for the largest value of  $L_0$ , the effective exponent is by about 4% and 6% larger than the asymptotically expected  $\nu = 0.6717(1)$ .

In the case of the improved model, leading corrections to scaling are due to the free boundary conditions. To take these into account we define an improved effective exponent as

$$\nu_{eff,\beta,L_s}(L_0) = -\ln\left(\frac{2L_0 + L_s}{L_0 + L_s}\right)/\ln\left(\frac{\beta_{KT}(2L_0) - \beta_{c,3d}}{\beta_{KT}(L_0) - \beta_{c,3d}}\right) . \quad (40)$$

Also here we define  $\nu_{eff,T,L_s}(L_0)$  by replacing  $\beta_{KT} - \beta_{c,3d}$  by  $T_{KT} - T_{c,3d}$  in eq. (40). Using  $L_s = 1.02$ , eq. (26), we arrive at the results that are plotted in figure 6.

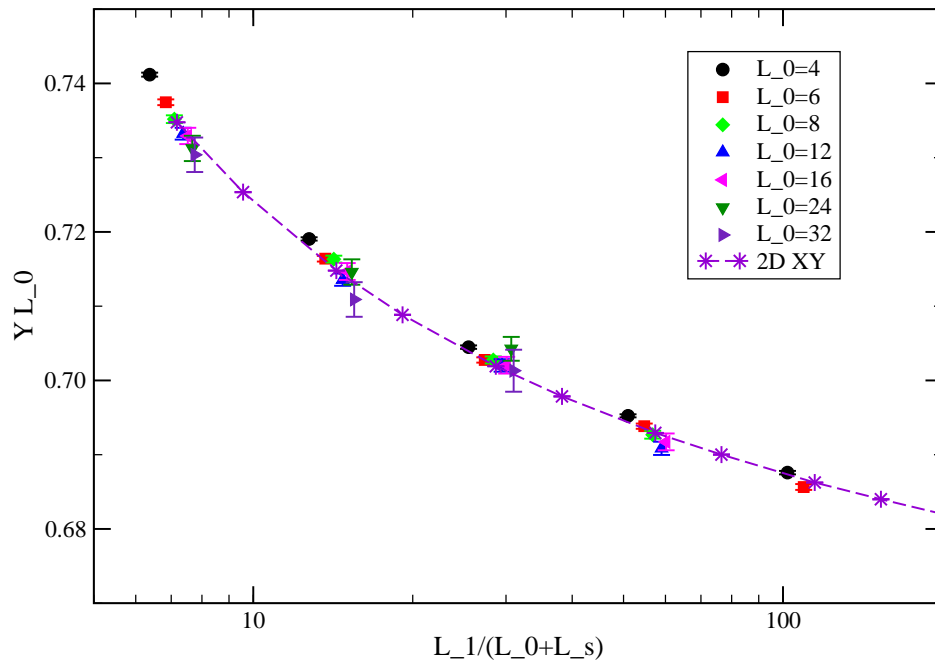
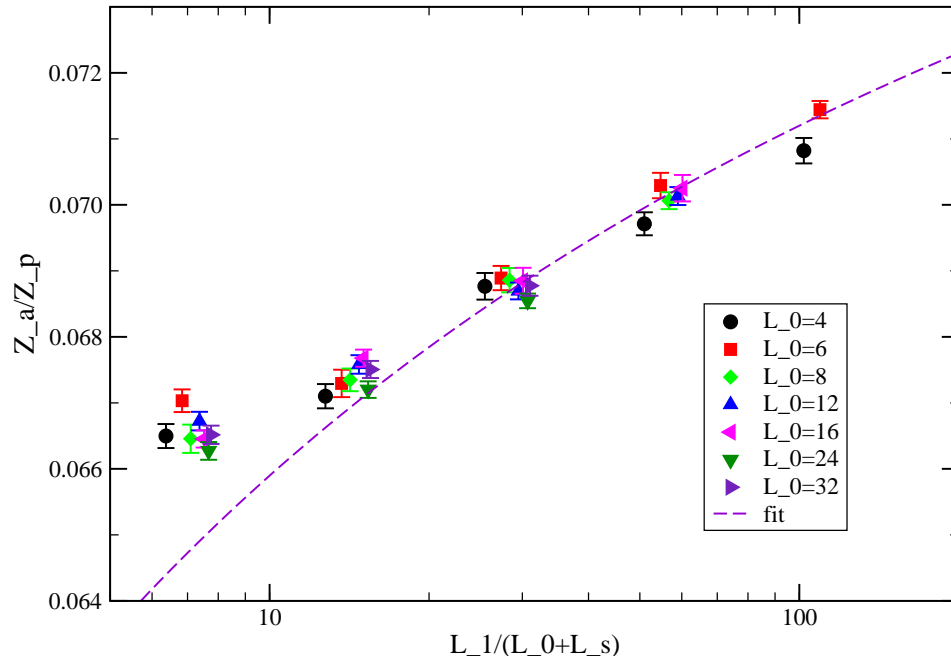


Figure 5: Effectively two-dimensional finite size scaling of  $Z_a/Z_p$  (upper part of the figure) and of  $L_0 Y$  (lower part of the figure). For a discussion see the text

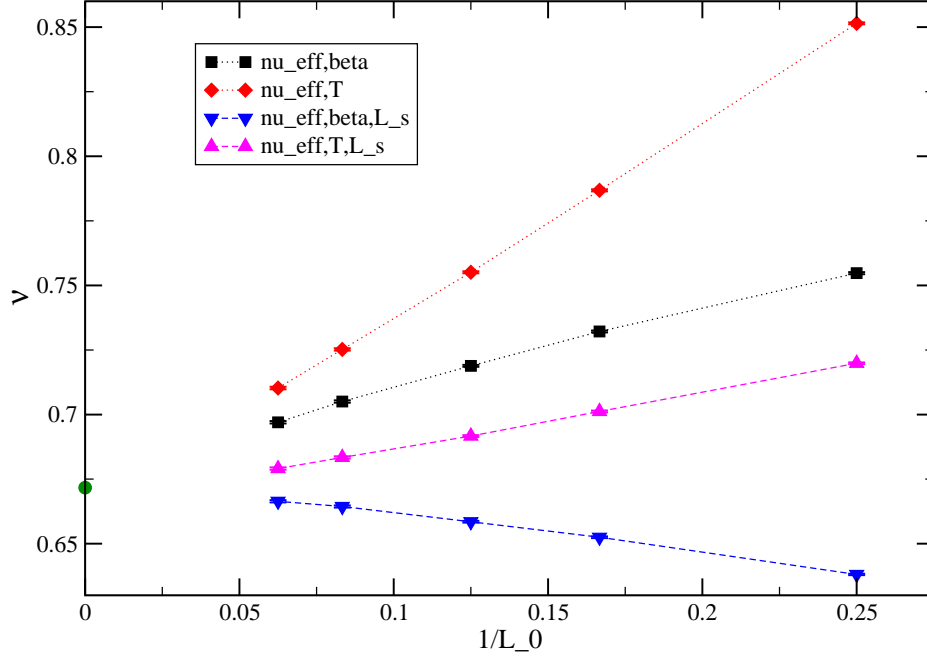


Figure 6: We plot the results for  $\nu_{\text{eff},\beta}(L_0)$ ,  $\nu_{\text{eff},T}(L_0)$ ,  $\nu_{\text{eff},\beta,L_s}(L_0)$  and  $\nu_{\text{eff},T,L_s}(L_0)$  as defined by eqs. (39,40) and the text below these equations. The green dot gives the most precise estimate  $\nu = 0.6717(1)$  [10] for the critical exponent of the correlation length of the 3D XY universality class. The dotted lines should only guide the eye.

Table 9: Results of fits with the ansatz (41).  $L_{0,min}$  is the minimal thickness that is taken into account. As discussed in the text,  $a$ ,  $L_s$  and  $c$  are the parameters of the fit.

$L_{0,min}$	$a$	$L_s$	$c$	$\chi^2/\text{d.o.f.}$
4	1.0321(11)	1.158(29)	1.38(11)	3.80
6	1.0286(13)	1.037(36)	0.90(13)	0.39
8	1.0284(18)	1.030(59)	0.87(23)	0.57

Table 10: Similar to table 9 but with the ansatz (42).

$L_{0,min}$	$\tilde{a}$	$L_s$	$\tilde{c}$	$\chi^2/\text{d.o.f.}$
4	3.9788(25)	1.118(11)	-0.851(24)	2.43
6	3.9697(35)	1.057(21)	-1.03(6)	0.43
8	3.9684(55)	1.047(37)	-1.07(11)	0.60

Now,  $\nu_{eff,\beta,L_s}$  is increasing with increasing  $L_0$ , while  $\nu_{eff,T,L_s}$  is decreasing. Now, for the largest value of  $L_0$ , the difference with  $\nu = 0.6717(1)$  is only about 1% in both cases. The remaining difference between  $\nu_{eff,\beta,L_s}$  and  $\nu_{eff,T,L_s}$  indicates that analytic corrections have to be taken into account. Therefore we have fitted our data for  $\beta_{KT}$  with the ansatz

$$\beta_{KT}(L_0) - \beta_{c,3D} = a(L_0 + L_s)^{-1/\nu} \times (1 + c(L_0 + L_s)^{-1/\nu}) , \quad (41)$$

where we have included the leading analytic correction in addition to the correction caused by the boundaries. We take  $a$ ,  $L_s$  and  $c$  as free parameters of the fit, while now  $\beta_{c,3D} = 0.5091503$  and  $\nu = 0.6717$  are fixed. I.e. here we assume the RG prediction for the exponent to be correct. We have not included corrections  $\propto L^{-\omega}$  since for  $\lambda = 2.1$  the amplitude of these corrections should be small. Furthermore it should be difficult to disentangle them from the boundary corrections which are  $\propto L_0^{-1}$ . The results of these fits are given in table 9. Next we have repeated the fit, replacing  $\beta$  by  $T$  in the ansatz (41):

$$T_{c,3D} - T_{KT}(L_0) = \tilde{a}(L_0 + L_s)^{-1/\nu} \times (1 + \tilde{c}(L_0 + L_s)^{-1/\nu}) . \quad (42)$$

For both types of fits we find  $\chi^2/\text{d.o.f.} < 1$  already for  $L_{0,min} = 6$ , where we have included all data with  $L_0 \geq L_{0,min}$  into the fit. The result for  $L_s$  from the fits

with  $L_{0,min} = 6$  and  $8$  are compatible among each other. Furthermore they are in perfect agreement with the result  $L_s = 1.02(7)$ , eq. (26), obtained from FSS at  $\beta_{c,3d}$ . Also the results for the leading amplitude are compatible among the two types of fits: Using  $a = \tilde{a}\beta_c^2$  we convert the results of  $\tilde{a}$  given in table 10 to  $a = 1.0314(6)$ ,  $1.0291(9)$  and  $1.0287(14)$  for  $L_{0,min} = 4, 6$  and  $8$ , respectively. I.e. the difference between the two types of fits is negligible.

We take our final result for the amplitude from the fit with ansatz (41) and  $L_{0,min} = 8$ . We have repeated this fit for shifted values of the input parameters: for  $\beta_{c,3d} = 0.5091509$ ,  $\nu = 0.6717$  and for  $\beta_{c,3d} = 0.5091503$ ,  $\nu = 0.6718$ . From the results of these fits we conclude for the amplitude

$$a = 1.028(2) - 10.5 \times (\nu - 0.6717) - 400 \times (\beta_{c,3d} - 0.5091503) . \quad (43)$$

The analysis of the behaviour of  $\beta_{KT}$  presented in this section leaves little doubt that the finite size scaling prediction (3,38) is correct. To fit data for thicknesses in the range  $6 \leq L_0 \leq 32$  properly, boundary corrections and leading analytic corrections have to be taken into account. Note that in the case of models which are not improved, also corrections  $\propto L_0^{-\omega}$  should play a role.

## 7.2 Universal amplitude ratios

As we have noted already in the introduction, finite size scaling predicts that the KT transition should occur at a universal value of  $L_0/\xi$ , where  $\xi$  is a correlation length of the three-dimensional bulk system. In this section we shall compute this ratio, using the transversal correlation length  $\xi_{\perp} = 1/\Upsilon$  and the second moment correlation length  $\xi_{2nd}$  in the high temperature phase.

For the following discussion it is more convenient to consider the inverse of the function  $\beta_{KT}(L_0)$ , namely the thickness  $L_{0,KT}(\beta)$  where the KT transition occurs at a given value of  $\beta$ . Of course this is not well defined, since  $L_0$  can take only integer values, and therefore for almost all values of  $\beta$  there is no such  $L_0$ . However by proper interpolation this problem can be solved, at least on a practical level.

There are several strategies to compute the universal amplitude ratios from Monte Carlo data. For a discussion see e.g. ref. [50]. If both quantities live in the same phase, as it is the case here for  $L_{0,KT}$  and  $\Upsilon$ , we can simply consider the product at the same value of  $\beta$ , or equivalently the same temperature  $T$ . Then the critical limit is taken

$$[L_{0,KT}\Upsilon]^* \equiv \lim_{\beta \rightarrow \beta_{c,3d}} L_{0,KT}(\beta)\Upsilon(\beta) . \quad (44)$$

One expects from RG theory that the approach to the critical limit is described by

$$(L_{0,KT} + L_s)\Upsilon = [L_{0,KT}\Upsilon]^* + cL_{0,KT}^{-\omega} + \dots . \quad (45)$$

If the two quantities live in different phases, as it is the case here for  $L_{0,KT}$  and  $\xi_{2nd}$  in the high temperature phase, we define

$$[L_{0,KT}/\xi_{2nd}]^* \equiv \lim_{\beta \rightarrow \beta_{c,3d}} L_{0,KT}(\beta)/\xi_{2nd}(2\beta_{c,3d} - \beta) . \quad (46)$$

I.e. the two quantities are taken at the same distance from the critical point of the three-dimensional system. This is however not uniquely defined. Instead of the same distance in  $\beta$  we could also use the same distance in  $T$ . Therefore, in contrast to eq. (45) also analytic corrections appear

$$(L_{0,KT}(\beta) + L_s)/\xi_{2nd}(2\beta_{c,3d} - \beta) = [L_{0,KT}/\xi_{2nd}]^* + cL_{0,KT}^{-\omega} + \dots + dL_{0,KT}^{-1/\nu} + \dots . \quad (47)$$

The universal ratio can also be expressed in terms of amplitudes:

$$[L_{0,KT}/\xi_{2nd}]^* = a^\nu f_{2nd,+}^{-1} , \quad (48)$$

where  $a$  is defined by eq. (41) and  $f_{2nd,+}$  is the amplitude of the second moment correlation length in the high temperature phase.

### 7.2.1 The second moment correlation length in the high temperature phase

Here we analyse the Monte Carlo data for  $\xi_{2nd}$  given in table 5 of ref. [12]. We have fitted these data with the ansatz

$$\xi_{2nd} = f_{2nd,+}(\beta_{c,3d} - \beta)^{-\nu} \times [1 + b(\beta_{c,3d} - \beta)^\Delta + c(\beta_{c,3d} - \beta)] , \quad (49)$$

where we have included leading corrections  $\propto (\beta_c - \beta)^\Delta$  and analytic corrections. We have fixed  $\nu = 0.6717$ ,  $\beta = 0.5091503$  and  $\Delta = \nu\omega = 0.527$ , given in ref. [10]. The results of these fits are summarized in table 11. A  $\chi^2/\text{d.o.f.}$  close to one is reached for  $\beta_{min} = 0.485$ . The result for  $f_{2nd,+}$  shows very little dependence on  $\beta_{min}$ . Therefore we take as our final result the one for  $\beta_{min} = 0.49$ :

$$f_{2nd,+} = 0.26362(8) + 223 \times (\beta_{c,3d} - 0.5091503) - 2.1 \times (\nu - 0.6717) , \quad (50)$$

where we have obtained the dependence on  $\beta_{c,3d}$  and on  $\nu$  by redoing the fits with slightly changed values of  $\beta_{c,3d}$  and  $\nu$ .

Table 11: *Fitting  $\xi_{2nd}$  in the high temperature phase of the three-dimensional  $\phi^4$  model at  $\lambda = 2.1$  with the ansatz (49). All data with  $\beta \geq \beta_{min}$  are taken into account.*

$\beta_{min}$	$f_{2nd,+}$	$b$	$c$	$\chi^2/\text{d.o.f.}$
0.48	0.26352(5)	0.050(4)	-0.77(2)	1.54
0.485	0.26359(6)	0.043(5)	-0.73(2)	1.14
0.49	0.26362(8)	0.039(8)	-0.72(4)	1.23

Now we can compute the universal ratio by using the results (43,50):

$$[L_{0,KT}/\xi_{2nd}]^* = a^\nu f_{2nd,+}^{\nu-1} = 3.864(6) - 4300(\beta_{c,3d} - 0.5091503) + 5(\nu - 0.6717) . \quad (51)$$

Note that the error of this product is mainly due to the error of  $a$ . Taking into account the uncertainty in  $\beta_c$  and  $\nu$  we arrive at

$$[L_{0,KT}/\xi_{2nd}]^* = 3.864(9) . \quad (52)$$

One should note that the exponential correlation length  $\xi_{exp}$ , which describes the asymptotic decay of the correlation function, differs only slightly from  $\xi_{2nd}$  which has been used here. Following ref. [40]:

$$\lim_{\beta \rightarrow \beta_{c,3d}} \frac{\xi_{exp}}{\xi_{2nd}} = 1.000204(3) , \quad (\beta < \beta_{c,3d}) . \quad (53)$$

Hence at the level of our accuracy this difference plays no role.

### 7.2.2 The helicity modulus in the low temperature phase

The results for the helicity modulus, which are summarized in the second column of table 12, are taken from ref. [12]. In order to obtain  $L_{0,KT}(\beta)$  at the values of  $\beta$  that were simulated in ref. [12], we have to interpolate the results given in table 8. To this end we have used the ansatz (41) along with the values for the coefficients obtained from the fit with  $L_{0,min} = 8$ . The numbers for  $L_{0,KT}(\beta)$  that are given in the third column of table 12 are obtained by numerically inverting eq. (41). Note that for the present purpose, the asymptotic correctness of the coefficients of eq. (41) is less important. For the present purpose it is sufficient that the function accurately describes our data in the range of  $L_0$  that has been simulated. In table



Table 12: Results for the product  $L_{0,KT}(\beta)\Upsilon(\beta)$

$\beta$	$\Upsilon$	$L_{0,KT}$	$L_{0,KT}\Upsilon$	$(L_{0,KT} + L_s)\Upsilon$
0.515	0.04939(8)	31.29	1.5454(25)[8]	1.5958(26)[8]{35}
0.52	0.07456(7)	20.37	1.5187(14)[8]	1.5948(15)[8]{52}
0.525	0.09628(7)	15.61	1.5029(11)[8]	1.6011(12)[8]{67}
0.53	0.11565(7)	12.845	1.4855(9)[7]	1.6035(10)[8]{81}
0.535	0.13349(6)	11.012	1.4670(7)[7]	1.6062(7)[8]{93}
0.54	0.15035(6)	9.692	1.4572(6)[7]	1.6105(6)[8]{105}
0.55	0.18145(6)	7.895	1.4325(5)[7]	1.6176(5)[8]{127}
0.58	0.26340(5)	5.229	1.3773(3)[7]	1.6460(3)[8]{184}

12 we quote no error for  $L_{0,KT}$ . Given the accuracy of  $\beta_{KT}(L_0)$  we expect an relative error of about 1/2 ‰ for  $L_{0,KT}$  at a fixed value of  $\beta$ .

In the fourth column of table 12 we have computed the product  $L_{0,KT}(\beta)\Upsilon(\beta)$ ; in ( ) we give the error due to the error of  $\Upsilon$  and in [] the 1/2 ‰ error assumed for  $L_{0,KT}(\beta)$ .  $L_{0,KT}(\beta)\Upsilon(\beta)$  is increasing with decreasing  $\beta$ . Even for the two smallest values of the inverse temperature  $\beta = 0.52$  and  $\beta = 0.515$ , the difference of  $L_{0,KT}(\beta)\Upsilon(\beta)$  is larger than the error. In order to take into account the boundary corrections, which are leading for the improved model, we have computed  $(L_{0,KT} + L_s)\Upsilon$ . The results are given in the last column of table 12. We have used the numerical value  $L_s = 1.02(7)$ , eq. (26). The error of  $L_s$  is reflected by the number given in {}. Now the dependence of the product on  $\beta$  is much reduced. Starting from  $\beta = 0.53$ , the results are consistent within the quoted errors. As our final result we take

$$[L_{0,KT}\Upsilon]^* = 1.595(7) \quad (54)$$

which is the average of the result for  $\beta = 0.515$  and 0.52. The error-bar includes all results up to  $\beta = 0.53$ . For illustration we have plotted in fig. 7 the results given table 12 along with our final result (54).

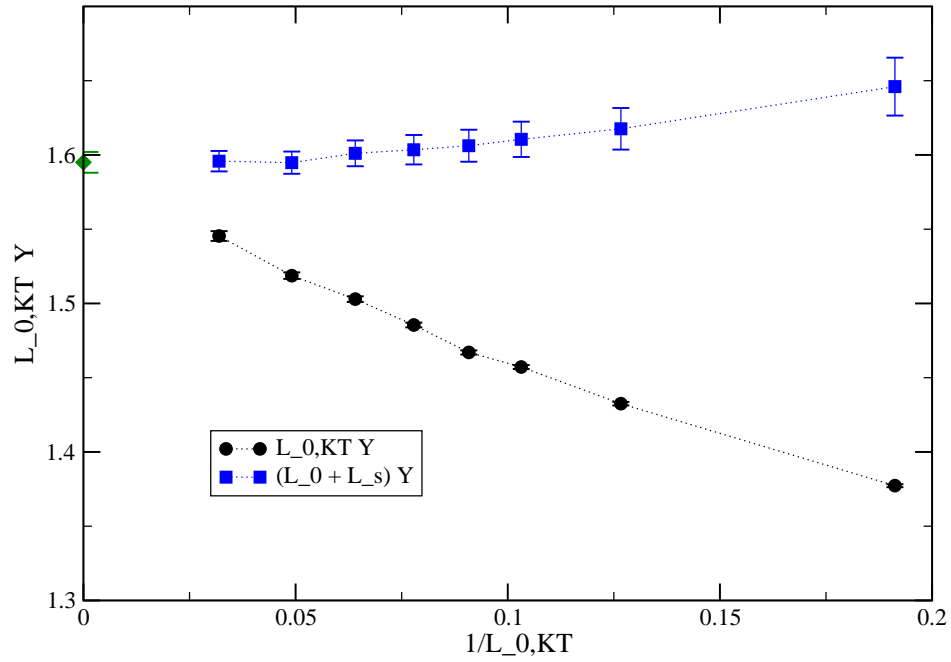


Figure 7: The numerical estimates of  $L_{0,KT}\Upsilon$  and  $(L_{0,KT} + L_s)\Upsilon$  which are quoted in table 12 are plotted as a function of  $1/L_{0,KT}$ . In addition we give our final result (54) (green diamond) for the limit  $L_{0,KT} \rightarrow \infty$ . For a discussion see the text.

Table 13: Preliminary estimates of  $\beta_{KT}$  for the dynamically diluted XY model at  $D = 1.02$ . The results are all obtained from lattices of the size  $L_1 = L_2 = 16 \times L_0$  by requiring  $\xi_{2nd}/L = 0.792(2)$ . For a discussion see the text.

$L_0$	$\beta_{KT}$
4	0.6767(3)[2]
8	0.60871(14)[6]
16	0.58083(11)[3]
32	0.57012(3)[2]

## 8 Preliminary results for the dynamically diluted XY model and the standard XY model

We have performed a preliminary study of the dynamically diluted XY model at  $D = 1.02$  and the standard XY model. To this end we have simulated lattices of the size  $L_1 = L_2 = 16 \times L_0$  with  $L_0 = 4, 8, 16$  and  $32$ . In order to determine  $\beta_{KT}$  we assume that effectively two-dimensional finite size effects are universal in thin films in the 3D XY universality class. I.e. that they are the same as for the  $\phi^4$  model studied in section 7. In particular we read off from figure 4 that  $\xi_{2nd}/L = 0.792(2)$  for  $L_1/L_0 = 16$  at the KT transition temperature. In the following we have determined an estimate of  $\beta_{KT}$  by requiring that  $\xi_{2nd}/L$  assumes the value  $0.792$  on lattices with  $L_1/L_0 = 16$ . The results obtained this way are summarized in table 13 for the dynamically diluted XY model at  $D = 1.02$  and in table 14 for the standard XY model. The number given in  $()$  is the statistical error, while the number given  $[\ ]$  is the error due to the uncertainty of  $\xi_{2nd}/L$ .

As a consistency check we have computed  $L_0\Upsilon$  and  $U_4$  at the values of  $\beta_{KT}$  summarized in tables 13 and 14. Indeed we find that  $U_4 \approx 1.02$  and  $L_0\Upsilon \approx 0.715$  as we also read off for  $L_1/L_0 = 16$  from figures 4 and 5 for the  $\phi^4$  model, respectively.

The results for the ddXY model, including all data, can be fitted by

$$\text{ddXY, } D = 1.02 : \quad \beta_{KT} = 0.5637963 + 1.1286(71) \times (L_0 + 0.70(3))^{-1/0.6717} . \quad (55)$$

Since we have only data for a few thicknesses of the film, we cannot check for systematic errors due to subleading corrections.

In table 14, for the standard XY model we also give the results that can be found in table I of ref. [30] which were obtained with staggered boundary conditions.

Table 14: Preliminary results for  $\beta_{KT}$  for the standard XY model are summarized in the second column. In the third column we give for comparison the results obtained in ref. [30]. Note that these refer to staggered boundary conditions and therefore no exact match of the numbers is expected.

$L_0$	$\beta_{KT}$ , ours	$\beta_{KT}$ , [30]
4	0.5665(3)[3]	0.5448(3)
8	0.4987(2)[1]	0.4949(10)
12		0.47934(23)
16	0.47132(3)[3]	0.47226(7)
20		0.46847(15)
32	0.46050(2)[1]	

Therefore no exact match with our results is expected. For  $L_0 = 4$  the inverse KT transition temperature  $\beta_{KT}$  of ref. [30] is clearly smaller than ours. For  $L_0 = 8$  it is still slightly smaller, while for  $L_0 = 16$  it is slightly larger than ours.

Fitting the results for the standard XY model is more difficult than those of the ddXY model at  $D = 1.02$ , since for the standard XY model we expect a sizable correction  $\propto L^{-\omega}$  with  $\omega \approx 0.785(20)$  [10]. Ignoring these corrections we get from fitting all our data of table 14

$$\text{XY : } \quad \beta_{KT} = 0.4541655 + 1.1387(45) \times (L_0 + 0.75(2))^{-1/0.6717} \quad (56)$$

with  $\chi^2/\text{d.o.f.} = 2.02$ . Taking into account the correction  $\propto L^{-\omega}$  instead of the boundary correction we obtain

$$\text{XY : } \quad \beta_{KT} = 0.4541655 + 1.1545(46) \times (1 - 0.70(2) \times L_0^{-0.785}) \times L_0^{-1/0.6717} \quad (57)$$

with  $\chi^2/\text{d.o.f.} = 1.92$ . Given the small number of data points available we made no attempt to fit both types of corrections simultaneously. The difference between the two fits (56,57) might give some indication of systematic errors.

Fitting the values of  $\beta_{KT}$  for  $L_0 = 8, 12, 16$  and  $20$  of ref. [30] we get

$$\beta_{KT, \text{staggered}} = 0.4541655 + 1.47(13) \times (L_0 + 3.13(76))^{-1/0.6717} \quad (58)$$

or alternatively, taking into account corrections  $\propto L_0^{-\omega}$ :

$$\beta_{KT, \text{staggered}} = 0.4541655 + 1.44(10) \times (1 - 1.92(25) \times L_0^{-0.785}) \times L_0^{-1/0.6717} . \quad (59)$$

If free and staggered boundary conditions are equivalent, the prefactor of  $L_0^{-1/0.6717}$  should be identical. Apparently, here we find a discrepancy of about three times the error. Based on the data of ref. [30] it is hard to decide whether this discrepancy is due to subleading corrections which are not taken into account or a subtle cancellation of corrections  $\propto L_0^{-\omega}$  and  $\propto L_0^{-1}$  or that free and staggered boundary conditions are, against our expectation, not equivalent.

In relation with ref. [10] we have also determined the correlation length of the standard XY model and the ddXY at  $D = 1.02$  in the high temperature phase. Using a similar analysis as for the  $\phi^4$  model at  $\lambda = 2.1$  in the previous section, we arrive at  $f_{2nd,+} = 0.2822(3)$  for the ddXY model at  $D = 1.02$  and  $f_{2nd,+} = 0.2880(3)$  for the standard XY model, where the amplitude  $f_{2nd,+}$  is defined by eq. (49). With eq. (51) we arrive at  $[L_{0,KT}/\xi_{2nd}]^* = 3.84(2)$  using eq. (55) for the ddXY model at  $D = 1.02$  and  $[L_{0,KT}/\xi_{2nd}]^* = 3.79(1)$  using eq. (56) and  $[L_{0,KT}/\xi_{2nd}]^* = 3.82(1)$  using eq. (57) for the standard XY model. Given the fact that systematic errors are not fully taken into account, we regard these results as consistent with our more precise estimate (52) obtained from the  $\phi^4$  model at  $\lambda = 2.1$ , confirming universality.

## 9 Comparison with experimental results

To our knowledge, there are no previous theoretical results for the amplitude ratios  $[L_{0,KT}\Upsilon]^*$  and  $[L_{0,KT}/\xi_{2nd}]^*$ .

The experimental study of  $^4\text{He}$  provides no access to the correlation length in the high temperature phase. On the other hand the helicity modulus can be computed from the superfluid density. Following ref. [42] the helicity modulus as defined here is given by

$$\Upsilon(T) = \frac{\hbar^2 \rho_{sb}(T)}{m^2 k_b T} \quad , \quad (60)$$

where  $\rho_{sb}(T)$  is the superfluid density of the bulk system and  $m$  the mass of a  $^4\text{He}$  atom. In the literature the inverse of the helicity modulus is called transverse correlation length  $\xi_T = 1/\Upsilon$ . The superfluid density can be obtained from measurements of the specific heat and the velocity of the second sound.

A number of experimental studies of the KT transition in thin films of  $^4\text{He}$  have been performed. For an overview see ref. [20]. Only a few of these works give results for the KT temperature, obtained e.g. from the onset of the superfluidity, for a sufficiently large range of the thickness of the film to extract a result for the universal combination  $[L_{0,KT}\Upsilon]^*$ . In fact in two of them an explicit result for  $[L_{0,KT}\Upsilon]^*$  is quoted:

Sabisky and Anderson [51] have performed experiments with films of  $^4\text{He}$  on various substrates. They have studied films of a thickness up to about  $75 \text{ \AA}$ . For films on  $\text{CaF}_2$  they find for  $L_0 \gtrsim 35 \text{ \AA}$  power law scaling of the film thickness with the reduced KT temperature with an exponent  $2/3$ , which is in reasonable agreement with the correlation length exponent  $\nu = 0.6717(1)$  [10]. Concerning the scaling of the thickness of the film with the superfluid density of the bulk system they write "the product  $(\rho_s/\rho)\xi(T) = 5.8T$  over the entire temperature range". In their notation  $\xi(T)$  is the thickness of the film where the KT transition takes place at the temperature  $T$ . It is clear from the text that Sabisky and Anderson have omitted a factor  $\text{\AA}/\text{K}$  on the right hand side of the equation. Plugging in numerical values for  $\rho$ ,  $\hbar$ ,  $m$  and  $T_\lambda$  into eq. (60) we arrive at

$$[L_{0,KT}\Upsilon]^* = 5.8 \times 0.2664 = 1.545 \quad . \quad (61)$$

The authors of ref. [52] have studied Helium films on glass of a thickness up to  $47 \text{ \AA}$ . They also find power law scaling of the KT thickness of the film with the temperature. Their numerical estimate for the exponent is  $0.71$ . Even more interesting, they quote in their eq. (7):

$$\delta_c(T) = 0.43 + 1.61\xi_\perp(T) \quad , \quad (62)$$

where  $\delta_c(T)$  is the KT thickness of the film at the temperature  $T$  and  $\xi_\perp(T)$  is the transverse correlation length of the bulk. I.e. they give a direct estimate for the universal combination which we are interested in. It matches perfectly with our theoretical result.

It is a bit puzzling that there are more recent experimental studies using larger thicknesses of the  $^4\text{He}$  film, which fit less well the theoretical expectation than the two reported above. Yu et al. [53] have studied  $^4\text{He}$  films on Kapton up to a thickness of  $156 \text{ \AA}$ . They see a power law scaling, starting from  $25 \text{ \AA}$ . However they find an exponent  $0.52(1)$  which is clearly smaller than  $\nu = 0.6717(1)$ . Furthermore, from their figure 3 it can be clearly seen that the ratio of  $\xi_\perp(T)$  and the KT thickness varies a lot over the range of thicknesses that has been studied. For their largest thickness,  $156 \text{ \AA}$  we read off from their figure  $L_{0,KT}/\xi_\perp \approx 10^{0.2} \approx 1.58$ . On the other hand, for  $25 \text{ \AA}$  one reads off  $L_{0,KT}/\xi_\perp \approx 10^{0.4} \approx 2.51$ . The reduced transition temperatures are  $0.2541$  and  $0.0073$  for  $25 \text{ \AA}$  and  $156 \text{ \AA}$ , respectively [54].

In refs. [55, 56] the KT temperature has been determined for films of the thickness  $483 \text{ \AA}$  and  $2113 \text{ \AA}$  at saturated vapour pressure. These films are confined by two wafers of silicon. The adiabatic fountain resonance method has been used to determine the KT transition temperature. The reduced transition temperatures

are  $\approx 1.29 \times 10^{-3}$  and  $\approx 1.64 \times 10^{-4}$  for 483 Å and 2113 Å, respectively [54]. An estimate of  $\xi_{\perp}$  can be obtained e.g. from ref. [7]: from their figure 3 we read off  $\xi_0 \approx 3.42$  Å at saturated vapour pressure, where  $\xi_{\perp} \simeq \xi_0 t^{-\nu}$ . It follows  $L_{0,KT}/\xi_{\perp} \approx 1.62$  and 1.77 for 483 Å and 2113 Å, respectively.

## 10 Summary and Conclusions

We have simulated lattice models in the three-dimensional XY universality class with thin film geometry. In order to mimic the vanishing order parameter at the boundaries that is observed in experiments on thin films of  ${}^4\text{He}$  we have implemented free boundary conditions. These boundary conditions lead to corrections to finite size scaling  $\propto L_0^{-1}$ , where  $L_0$  is the thickness of the film. These corrections can be described by  $L_{0,eff} = L_0 + L_s$ . Furthermore one expects corrections to finite size scaling  $\propto L_0^{-\omega}$  [16], where  $\omega = 0.785(20)$  [10]. Analysing Monte Carlo data, it is difficult to disentangle corrections with exponents that are so close. In fact in previous studies, e.g. [30], of thin films, using the standard XY model, only the boundary corrections have been taken into account, which might lead to systematic errors in the extrapolation to the critical limit. In order to avoid this problem, we have studied improved models. In particular we have studied in detail the  $\phi^4$  model on a simple cubic lattice at  $\lambda = 2.1$ . This value of the parameter  $\lambda$  is close to the most recent estimate  $\lambda^* = 2.15(5)$  [10], where  $\lambda^*$  is defined such that the amplitude of leading corrections exactly vanishes. At  $\lambda = 2.1$  the amplitude of corrections to scaling should be at least by a factor of 20 smaller than in the standard XY model.

First we have studied the  $\phi^4$  model at the critical point of three-dimensional system. We have simulated lattices of the size  $L_0 = L_1 = L_2$  and  $L_0 + 1 = L_1 = L_2$  with  $L_1 = 8, 12, 16, 24, 32$  and 48. We employed free boundary conditions in 0-direction, while periodic boundary conditions are employed in 1 and 2-direction. We have measured the four phenomenological couplings  $U_4$ ,  $U_6$ ,  $\xi_{2nd}/L$  and  $Z_a/Z_p$ . The latter two quantities are taken only for the 1 and the 2-direction. We clearly see corrections  $\propto L_0^{-1}$  in all of these quantities. This is in clear contrast with simulations, where periodic boundary conditions in all directions are employed. E.g. in ref. [10], using improved models one sees corrections  $\propto L_0^{-\epsilon}$ , where  $1.6 \lesssim \epsilon \lesssim 2$ . Casting the corrections  $\propto L_0^{-1}$  into the form  $L_{0,eff} = L_0 + L_s$ , one gets, within the error, the *same* value for  $L_s$  from all four quantities. As our final result we quote  $L_s = 1.02(7)$ . Note that  $L_s$  depends on the model and on the particular boundary conditions that are used. In future studies of other properties of thin films, like e.g. the thermodynamic Casimir force, using the same lattice model as here, the

knowledge of  $L_s$  is a valuable asset.

Next we studied the phase transition in thin films. To this end, we applied a finite size scaling method that we have proposed recently [34]. Finite size scaling of the effectively two-dimensional film means  $L_0 \ll L_1, L_2 \lesssim \xi$ , where  $\xi$  is the correlation length in the 1 or 2-direction of a system with the thickness  $L_0$  and infinite extension in the other two directions. Also here, we have studied in detail the  $\phi^4$  model at  $\lambda = 2.1$ . We have simulated lattices up to  $L_1/L_0 = 128$  for  $L_0 = 4$  and 6, up to  $L_1/L_0 = 64$  for  $L_0 = 8, 12$  and 16 and up to  $L_1/L_0 = 32$  for  $L_0 = 24$  and 32. Matching the finite size behaviour of the second moment correlation length  $\xi_{2nd}/L$  and the Binder cumulant  $U_4$  with that of the dual of the ASOS model at the Kosterlitz-Thouless (KT) transition we obtain accurate estimates of the transition temperature of the thin films. Note that the finite size scaling behaviour is very similar for different two-dimensional XY models [34]. The dual of the ASOS model has been chosen in ref. [34] as reference model for purely technical reason. Furthermore, we obtain an estimate for the scale factor  $b_{ASOS, film}$  that relates the effective two-dimensional lattice size  $L_1/L_0$  of the thin film and that of the dual of the ASOS model. The finite size scaling behaviour of  $Z_a/Z_p$  and the helicity modulus times the thickness  $L_0\Upsilon$ , which were not used to determine  $\beta_{KT}$  and  $b_{ASOS, film}$ , clearly confirm the KT nature of the transition in the thin films.

Next we have studied the scaling of the inverse of the KT temperature  $\beta_{KT}$  with the thickness  $L_0$  of the film. We find that for the thicknesses that we have studied, even in the improved model, corrections to scaling are important. Using the ansatz (41) that includes corrections due to the free boundary conditions as well as leading analytic corrections we can fit, fixing  $\nu = 0.6717(1)$ , all data with  $L_0 \geq 6$ , with  $\chi^2/\text{d.o.f.} = 0.39$ .

For the first time, we provide a theoretical estimate for the amplitude ratio

$$[L_{0,KT}/\xi_{\perp}]^* = 1.595(7) \quad , \quad (63)$$

where  $\xi_{\perp}$  is the transversal correlation length in the low temperature phase of the three-dimensional bulk system. Note that  $\xi_{\perp}$  is the inverse of the helicity modulus as defined here. This result nicely compares with the experimental results of refs. [51, 52]. On the other hand, more recent experiments [55, 56] on  $^4\text{He}$  films with thicker films seem to match less well.

We have also computed the universal amplitude ratio  $[L_{0,KT}/\xi_{2nd}]^* = 3.864(9)$ , where  $\xi_{2nd}$  is the second moment correlation length of the three-dimensional bulk system in the high temperature phase. We also provide some preliminary results for the KT transition temperature for the dynamically diluted XY model at  $D = 1.02$



and the standard XY model for  $L_0 = 4, 8, 16$  and  $32$ . Using the data of these two models we get results for  $[L_{0,KT}/\xi_{2nd}]^*$  that are essentially consistent with the one quoted above for the  $\phi^4$  model, confirming the universality of the result.

## 11 Appendix A: Ratio of partition functions $Z_a/Z_p$ at the KT transition

In the spin-wave approximation of a two-dimensional XY model, the partition function is given by

$$Z_{SW} = \sum_{n_1, n_2} W(n_1, n_2) Z(0, 0) \quad , \quad (64)$$

where  $n_1$  and  $n_2$  count the windings of the XY field along the 1 and 2 directions. In the case  $L_1 = L_2$ , for isotropic couplings, the weights are given by

$$W(n_1, n_2) = \exp\left(-2\pi^2\beta_{SW}[n_1^2 + n_2^2]\right) \quad , \quad (65)$$

where for periodic boundary conditions,  $n_1$  and  $n_2$  take integer values and in the case of antiperiodic boundary conditions half-integer. I.e. in the spin-wave approximation

$$\frac{Z_a}{Z_p} = \frac{\sum_{n_1=-\infty}^{\infty} \sum_{n_2=-\infty}^{\infty} \exp\left(-2\pi^2\beta_{SW}[(n_1 + 1/2)^2 + n_2^2]\right)}{\sum_{n_1=-\infty}^{\infty} \sum_{n_2=-\infty}^{\infty} \exp\left(-2\pi^2\beta_{SW}[n_1^2 + n_2^2]\right)} \quad . \quad (66)$$

The KT transition is characterized by  $\beta_{SW} = 2/\pi$ . For the neighbourhood of the KT transition we get

$$Z_a/Z_p = 0.0864272337\dots - 0.426489404\dots(\beta - 2/\pi) + \dots \quad . \quad (67)$$

At the KT transition the  $\beta_{SW}$  depends on the scale as

$$\beta_{SW} = 2/\pi + \frac{1}{\pi} \frac{1}{\ln L + C} + \dots \quad , \quad (68)$$

where in finite size scaling, we identify this scale with the lattice size. It follows for lattices with  $L_1 = L_2 = L$ :

$$Z_a/Z_p = 0.0864272337\dots - 0.135755793\dots \frac{1}{\ln L + C} + \dots \quad . \quad (69)$$

## 12 Acknowledgements

I like thank W. Janke for discussions and encouragement. Thanks to E. Vicari for reading the final version of the draft. I am grateful to M. Kimball for remarks on the status of experiments and for providing me with explicit results for reduced KT transition temperatures. This work was supported by the Deutsche Forschungsgemeinschaft (DFG) under grant No JA 483/23-1.

## References

- [1] Wilson K G and Kogut J, *The renormalization group and the  $\epsilon$ -expansion*, 1974 Phys. Rep. C **12** 75
- [2] Fisher M E, *The renormalization group in the theory of critical behavior*, 1974 Rev. Mod. Phys. **46** 597
- [3] Fisher M E, *Renormalization group theory: Its basis and formulation in statistical physics*, 1998 Rev. Mod. Phys. **70** 653
- [4] Pelissetto A and Vicari E, *Critical Phenomena and Renormalization-Group Theory*, 2002 Phys. Rept. **368** 549 [cond-mat/0012164]
- [5] Lipa J A, Swanson D R, Nissen J A, Chui T C P and Israelsson U E, *Heat Capacity and Thermal Relaxation of Bulk Helium very near the  $\lambda$ -Point*, 1996 Phys. Rev. Lett. **76** 944
- [6] Lipa J A, Nissen J A, Stricker D A, Swanson D R and Chui T C P, *Specific heat of liquid helium in zero gravity very near the  $\lambda$ -point*, 2003 Phys. Rev. B **68** 74518 [cond-mat/0310163]
- [7] Singasaas A and Ahlers G, *Universality of static properties near the superfluid transition in  $^4\text{He}$* , 1984 Phys. Rev. B **30** 5103
- [8] Goldner L S and Ahlers G, *Superfluid fraction of  $^4\text{He}$  very close to  $T_\lambda$* , 1992 Phys. Rev. B **45** 13129
- [9] Barmatz M, Hahn I, Lipa J A, and Duncan R V, *Critical phenomena in microgravity: Past, present, and future*, 2007 Rev. Mod. Phys. **79** 1

- [10] Campostrini M, Hasenbusch M, Pelissetto A, and Vicari E, *Theoretical estimates of the critical exponents of the superfluid transition in He4 by lattice methods*, 2006 Phys. Rev. B **74** 144506 [cond-mat/0605083]
- [11] Hasenbusch M, *The three-dimensional XY universality class: A high precision Monte Carlo estimate of the universal amplitude ratio  $A_+/A_-$* , 2006 J. Stat. Mech. P08019 [cond-mat/0607189]
- [12] Hasenbusch M, *A Monte Carlo study of the three-dimensional XY universality class: Universal amplitude ratios*, [arXiv:0810.2716]
- [13] Kosterlitz J M and Thouless D J, *Ordering, metastability and phase transitions in two-dimensional systems* 1973 J. Phys. C **6** 1181; Kosterlitz J M, *The critical properties of the two-dimensional xy model*, 1974 J. Phys. C **7** 1046 ne- or Two-Dimensional
- [14] José J V, Kadanoff L P, Kirkpatrick S and Nelson D R, *Renormalization, vortices, and symmetry-breaking perturbations in the two-dimensional planar model*, 1977 Phys. Rev. B **16** 1217
- [15] Amit D J, Goldschmidt Y Y and Grinstein G, *Renormalisation group analysis of the phase transition in the 2D Coulomb gas, Sine-Gordon theory and XY model*, 1980 J. Phys. A **13** 585
- [16] M. N. Barber *Finite-size Scaling in Phase Transitions and Critical Phenomena, Vol. 8*, eds. C. Domb and J. L. Lebowitz, (Academic Press, 1983)
- [17] *Finite Size Scaling and Numerical Simulation of Statistical Systems*, ed. V. Privman, (World Scientific, 1990).
- [18] M.E. Fisher, *Critical Phenomena*, Proceedings of the International School of Physics "Enrico Fermi, Varenna, Italy, Course LI, edited by M.S. Green (Academic, New York, 1971)
- [19] Capehart T W and Fisher M E, *Susceptibility scaling functions for ferromagnetic Ising films*, 1976 Phys. Rev. B **13** 5021
- [20] Gasparini F M, Kimball M O, Mooney K P, and Diaz-Avila M, *Finite-size scaling of  $^4\text{He}$  at the superfluid transition*, 2008 Rev. Mod. Phys. **80** 1009
- [21] Dohm V, *The superfluid transition in confined  $^4\text{He}$ : Renormalization-group theory*, 1993 PHYSICA SCRIPTA **T49A** 46.

- [22] Nho K and Manousakis E, *Heat-capacity scaling function for confined superfluids*, 2003 Phys. Rev. B **68** 174503 [cond-mat/0305500]
- [23] K. Binder, *Critical behaviour at surfaces in Phase Transitions and Critical Phenomena*, Vol. 8, eds. C. Domb and J. L. Lebowitz, (Academic Press, 1983) p. 1.
- [24] H. W. Diehl, Field-theoretical Approach to Critical Behaviour at Surfaces in *Phase Transitions and Critical Phenomena*, edited by C. Domb and J.L. Lebowitz, Vol. 10 (Academic, London 1986) p. 76.
- [25] Diehl H W, Dietrich S, and Eisenriegler E, *Universality, irrelevant surface operators, and corrections to scaling in systems with free surfaces and defect planes*, 1983 Phys. Rev. B **27** 2937
- [26] Newman K E and Riedel E K, *Critical exponents by the scaling-field method: The isotropic N-vector model in three dimensions*, 1984 Phys. Rev. B **30** 6615
- [27] Janke W and Nather K, *Monte Carlo simulation of dimensional crossover in the XY model*, 1993 Phys. Rev. B **48** 15807
- [28] Schultka N and Manousakis E, *Crossover from Two- to Three-Dimensional Behavior in Superfluids*, 1995 Phys. Rev. B **51** 11712 [cond-mat/9406014]
- [29] Schultka and E. Manousakis, *Scaling of the superfluid density in superfluid films*, 1996 J. Low. Temp. Phys. **105** 3 [cond-mat/9602085]
- [30] Schultka N and Manousakis E, *Boundary effects in superfluid films*, 1997 J. Low. Temp. Phys. **109** 733 [cond-mat/9702216]
- [31] Zhang C, Nho K, and Landau D P, *Finite-size effects on the thermal resistivity of  $^4\text{He}$  in the quasi-two-dimensional geometry*, 2006 Phys. Rev. B **73** 174508
- [32] Hucht A, *Thermodynamic Casimir Effect in  $^4\text{He}$  Films near  $T_c$ : Monte Carlo Results*, 2007 Phys. Rev. Lett. **99** 185301 [arXiv:0706.3458]
- [33] Vasilyev O, Gambassi A, Maciolek A, and Dietrich S, *Monte Carlo simulation results for critical Casimir forces*, 2007 Europhys. Lett. **80** 60009 [arXiv:0708.2902]
- [34] Hasenbusch M, *The Binder Cumulant at the Kosterlitz-Thouless Transition*, 2008 J. Stat. Mech. P08003 [arXiv:0804.1880]

- [35] Ballesteros H G, Fernandez L A, Martin-Mayor V, and Munoz-Sudupe A, *Finite size effects on measures of critical exponents in  $d=3$   $O(N)$  models*, 1996 Phys. Lett. B **387** 125 [cond-mat/9606203]
- [36] Cucchieri A, Engels J, Holtmann S, Mendes T and Schulze T, *Universal amplitude ratios from numerical studies of the three-dimensional  $O(2)$  model*, 2002 J. Phys. A **35** 6517 [cond-mat/0202017]
- [37] Deng Y, Blöte H W J, and Nightingale M P, *Surface and bulk transitions in three-dimensional  $O(n)$  models*, 2005 Phys. Rev. E **72** 016128 [cond-mat/0504173]
- [38] Bittner E and Janke W, *Nature of Phase Transitions in a Generalized Complex  $|\psi|^4$  Model*, 2005 Phys. Rev. B **71** 024512 [cond-mat/0501468]
- [39] Hasenbusch M and Török T, *High precision Monte Carlo study of the 3D XY-universality class*, 1999 J. Phys. A **32** 6361 [cond-mat/9904408]
- [40] Campostrini M, Hasenbusch M, Pelissetto A, Rossi P, and Vicari E, *Critical behavior of the three-dimensional XY universality class*, 2001 Phys. Rev. B **63** 214503 [cond-mat/0010360]
- [41] Li Y-H and Teitel S, *Finite-size scaling study of the three-dimensional classical XY model*, 1989 Phys. Rev. B **40** 9122
- [42] Fisher M E, Barber M N, and Jasnow D, *Helicity Modulus, Superfluidity, and Scaling in Isotropic Systems*, 1973 Phys. Rev. A **8** 1111
- [43] Hasenbusch M, *Direct Monte Carlo Measurement of the Surface Tension in Ising Models*, 1993 J. Phys. I (France) **3** 753 [hep-lat/9209016]
- [44] Wolff U, *Collective Monte Carlo Updating for Spin Systems*, 1989 Phys. Rev. Lett. **62** 361
- [45] Hasenbusch M, Pinn K and Vinti S, *Critical Exponents of the 3D Ising Universality Class From Finite Size Scaling With Standard and Improved Actions*, 1999 Phys. Rev. B **59** 11471 [hep-lat/9806012]
- [46] Saito M, *An Application of Finite Field: Design and Implementation of 128-bit Instruction-Based Fast Pseudorandom Number Generator*, PhD thesis, Dept.

of Math., Graduate School of Science, Hiroshima University, Advisor: M. Matsumoto; The numerical program and a detailed description can be found at “<http://www.math.sci.hiroshima-u.ac.jp/~m-mat/MT/SFMT/index.html>”

- [47] Weber H and Minnhagen P, *Monte Carlo determination of the critical temperature for the two-dimensional XY model*, 1988 Phys. Rev. B **37** 5986
- [48] Hasenbusch M, *The two-dimensional XY model at the transition temperature: A high precision Monte Carlo study*, 2005 J. Phys. A: Math. Gen. **38** 5869 [cond-mat/0502556]
- [49] Hasenbusch M and Pinn K, *Computing The Roughening Transition of Ising and Solid-on-Solid Models by BCSOS Model Matching*, 1997 J. Phys. A 30 (1997) 63 [cond-mat/9605019]
- [50] Caselle M and Hasenbusch M, *Universal Amplitude Ratios in the 3-D Ising Model*, 1997 J. Phys. A **30** 4963 [hep-lat/9701007]
- [51] Sabisky E S and Anderson C H, *Onset for Superfluid flow in He<sup>4</sup> Films on a Variety of Substrates*, 1973 Phys. Rev. Lett. **30** 1122
- [52] van de Laar R W A, van der Hoek A, van Beelen H, *Two-dimensional behaviour of very thin <sup>4</sup>He films on glass*, 1995 Physica B **216** 24.
- [53] Yu Y Y, Finotello D and Gasparini F M, *Finite-size scaling and the convective conductance and specific heat of planar helium films near the superfluid transition*, 1989 Phys. Rev. B **39** 6519
- [54] Kimball M O, private communication
- [55] Gasparini F M and Metha S *Temperature oscillations from a temperature superleak*, 1998 J. Low Temp. Phys. **110** 293
- [56] Kimball M O and Gasparini F M, *Superfluid fraction of He-3-He-4 mixtures confined at 0.0483  $\mu$  m between silicon wafers*, 2001 Phys. Rev. Lett. **86** 1558